Epithelial Factors Affecting Smooth Muscle Contraction of the Mouse Epididymis

Inaugural - Dissertation

zur Erlangung des Grades eines
Doktors der Zahnmedizin

des Fachbereichs Medizin

der Justus-Liebig-Universität Gießen

vorgelegt von Haas, Dirk Stefan

aus Frankfurt am Main

Gießen 2025

Aus dem Institut für Anatomie und Zellbiologie der
Humanmedizin der
Justus-Liebig-Universität Gießen

AG Signaltransduktion

Gutachter: Prof. Dr. Ralf Middendorff

Gutachter: PD. Dr. Bora Mustafa Altinkilic

Tag der Disputation: 11. November 2025

Table of Contents

1 Introduction

“Urinary tract infection (UTI) is some of the most common human bacterial infections” (Nickel 2019; Jhang and Kuo 2017; Wagenlehner et al. 2012; Werneburg et al. 2024) in urological clinics. UTI can be caused by bacteria in any part of the urinary system and ascend all the way up to the kidneys, or they may result in infertility (Stammler et al. 2015; Michel et al. 2015). The annual incidence of male patients is 3%, while the incidence in female patients is 12.6% (Jhang and Kuo 2017). The causes of the infection are numerous and varied (Jhang and Kuo 2017). The discrepancy in etiology between male and female cases can be attributed, among other factors, to the differing lengths of the routes of entry. To date, antibiotics remain the preferred treatment option (Nickel 2019; Wagenlehner et al. 2012; Nickel 2005). In female patients, antibiotic therapy is typically sufficient to achieve cure. However, the underlying pathology in males can be severe and is typically considered complex due to the high likelihood of progression to the kidneys. Consequently, some cases may necessitate surgical intervention.

The primary physiological functions of the epididymis have been identified as maturation, storage, and transport of spermatozoa (Elfgen et al. 2018; Mietens et al. 2014). However, the epididymis also plays a role in detecting and expelling foreign bodies, such as viruses or bacteria, in order to prevent ascending infections (Michel et al. 2015; Schütz et al. 2015).

The ductus epididymis of a mouse is approximately 1 m in length, whereas that of a human is 6 m (Hinton et al. 2011). It is composed of 10 segments (Jelinsky et al. 2007), which form the caput (segments 1-5), corpus (6-7), and cauda (8-10) of the epididymis (Jelinsky et al. 2007). It is covered by a pseudostratified cylindrical epithelium. The main cell types currently identified in the epididymis are as follows:

a) Principal cells (65-80%) (Trasler et al. 1988),
b) Basal cells (10-20%) (Trasler et al. 1988),
c) Apical cells (Robaire et al. 2015),
d) Narrow cells (Robaire et al. 2015),
e) Clear cells (3-10%) (Trasler et al. 1988),
f) Halo cells (3-10%) (Trasler et al. 1988).

Basal cells are present in all segments of the epididymis (Robaire and Hinton 2002; Trasler et al. 1988), and it is generally accepted that they do not reach the lumen. However, recent observations have indicated that some basal cells in the epididymal duct also reach the lumen, where they may function as luminal sensors (Shum et al. 2008).

Hinton posits that once the development of the epididymis is complete, there is no further proliferation. Hinton hypothesizes that this may be the reason for extremely low incidence of cancer in the epididymis (Hinton Speech 23 Nov. 2023 in Gießen).

In many organs, including the tongue (Avau et al. 2015; Schütz et al. 2015), trachea and lung (Krasteva et al. 2011), antrum, fundus, duodenum, and colon (Avau et al. 2015; Schütz et al. 2015), urethra (Deckmann et al. 2014), and testis (Xu et al. 2013), taste and taste-like receptors, e.g., Tas2r38 (for bitter sensing in human), Tas2r105, and particularly *Tas2r108* (Wu et al. 2005; Avau et al. 2015), were identified. Among others, they contain a *Tas2r108* receptor (Wu et al. 2005; Deckmann

et al. 2014; Avau et al. 2015), which reacts on ligands such as denatonium benzoate (Chandrashekar et al. 2000; Xu et al. 2013). The cells that express *Tas2r108* may also have a *Trpm5* cation channel (Hofmann et al. 2003), which is necessary for the transduction of bitter sensing (Clapp et al. 2001; Pérez et al. 2002; Zhang et al. 2003; Banik et al. 2018).

In other organs, bacteria trigger the aforementioned gustatory receptor-mediated signaling cascade, which may result in muscle contractions and ultimately serve as a protective mechanism (Deckmann et al. 2014; Krasteva-Christ et al. 2015; Deckmann et al. 2018). In 2017, Carrey et al. (2017) demonstrated that the "product(s) secreted by B. cereus induced nitric oxide (NO) production and increased ciliary beat frequency (CBF). The response exhibited notable inter-individual variability and involved two crucial components of bitter taste signaling, phospholipase C isoform β-2 and the transient receptor potential melastatin isoform 5 ion channel (*Trpm5*)." (Carey et al. 2017).

The data revealed by the mouse model of ascending infections (Stammler et al. 2015) allow for the presumption that bacteria in the lumen of the epididymal duct could affect the contractility of the smooth muscle layers surrounding the epithelium.

The present research, aimed to investigate the presence of taste receptor components of the gustatory signaling cascade in the epithelium of the epididymal duct and to determine whether signaling by the corresponding ligands such as denatonium benzoate triggers contraction of smooth muscle cells.

In her doctoral thesis, Ludmilla Dorscht demonstrated that *Tas2r108* receptors are present in the epididymis and that *Trpm5* ion channels are found in the epithelium but not in the smooth muscle layer (Dorscht 2020) (Figure 2-1).

The objective of this research is to identify cells in the epididymal duct that not only detect the invasion of foreign bodies but also trigger the contraction of smooth muscles to squeeze out invaders. This could potentially

prevent ascending infections and infertility and, thereby protect human evolution and species diversity.

1.1 Epididymis

1.1.1 Anatomy

The epididymis (derived from the Greek words epi, meaning “on top“ and didymos, meaning “double“, “twin“) (Figure 1-1) is a male genital organ that is connected dorsal to each of the two testes via the ducti efferentes testis. It primarily comprises a ductus epididymidis, which is approximately 6 m long in the human body. For comparison, the length of the ductus epididymidis of a mouse is approximately 1 m comprising 10 segments (Figure 1-3; Aumüller and Wurzinger 2010; Schünke et al. 2015). The twisted organ’s physiological length of the human epididymis is approximately 6 cm, whereas the epididymis of a mouse is approximately 5 mm in long. The epididymis is comprised of three primary sections (Figure 1-2 and Figure 1-3): caput, corpus, and cauda. The latter is connected to the ductus deferens. The tunica vaginalis testis provides cover for the epididymis. The two sheets, the outer periorchium and

the inner epiorchium, are connected to each other and together form the cavitas peritonealis scroti. The A. testicularis, the A. ductus deferentis, and the plexus pampiniformis are responsible for vascularization and sympathetic innervation (Ricker 1998). Lymphatic drainage is the responsibility of the NII. Lumbales and NII. Iliaci interni (Aumüller and Wurzinger 2010; Schünke et al. 2015). The ductus epididymis primarily houses immature (caput and corpus) and mature (cauda) spermatozoa, as well as essential hormones (e.g., androgen, estrogen, progesterone) (Leung et al. 1998), proteins (e.g., growth factors), and various cells that regulate the physiological environment (e.g., adjusting the pH value and temperature) in order to mature the spermatozoa's ability to fertilize ova. Furthermore, the ductus epididymis contains residual epithelial cells, macrophages, and fluid derived from the testis.

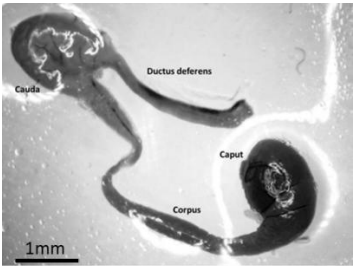

Figure 1-1: Photograph of a dissected epididymis

Source: Photograph taken by Haas.

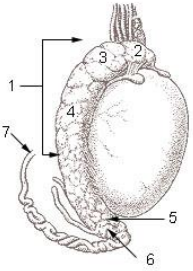

Figure 1-2: Raw structure of the epididymis

1 Epididymis, 2 Caput of epididymis, 3 Lobules of epididymis, 4 Corpus of epididymis, 5 Cauda of epididymis,

6 Duct of epididymis, 7 Deferent duct (also known as the ductus deferens and as the vas deferens)

Source: US Government 2006

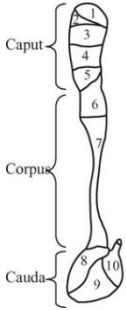

Figure 1-3: Segmental structure of the epididymis of a mouse

Segments 1-5 constitute the caput, including the initial segment,

6-7 the corpus, and

8-10 the cauda epididymidis.

The initial segment is defined by the first two segments (Domeniconi et al. 2016).

Source: Jelinsky et al. 2007

1.1.2 Function

The primary physiological functions of the epididymis are maturation (Bedford 1967), storage, and transport of spermatozoa (Mietens et al. 2014; Elfgen et al. 2018).

These are produced in the testis and reach the initial segment at the caput via the ductus efferentes. As immature spermatozoa are unable to move independently, the ductuli efferentes possess kinocilia on their epithelial surface and exhibit spontaneous contractions of the underlying smooth muscle layer to facilitate sperm transport. The microvilli on the epithelium's surface promote the resorption of fluid with an estimated 87% of the fluid being absorbed, thereby increasing the concentration of spermatozoa (Jones and Clulow 1987). The cauda is merged with the ductus deferens, which is connected to the urethra (Aumüller and Wurzinger 2010; Schünke et al. 2015). The ductus deferens, which is lined with a thick layer of smooth muscles, is responsible for transporting the mature spermatozoa during ejaculation. The total maturation and storage period in the distal part of the human epididymis is approximately 12 days on average (Bedford 1994). Men with high production rates have a transit time of approximately 2 days and a maturation time in caput and corpus of less than 2 days (Amann and Howards 1980). The total time required for the production of spermatozoa in the testis

and their subsequent transit through the epididymis is approximately 80 days (Schünke et al. 2015). The ductus epididymis and the ductus efferentes are derivatives of the Wolffian body (Robaire et al. 2015). Sympathetic innervation of the ductus deferens is maintained via the plexus testicularis, the plexus hypogastricus inferior, and the plexus deferentialis. The latter is responsible for the contraction of the ductus deferens, facilitating the transport of spermatozoa to a more distal location. The nervi splanchnici pelvici provide parasympathetic innervation (Schünke et al. 2015; Aumüller and Wurzinger 2010). The smooth muscles of the epididymis exhibit spontaneous contractions (Figure 3-2).

The pattern of spontaneous contractions demonstrates a decline in frequency from caput to cauda (Mewe et al. 2006a) (Figure 1-4).

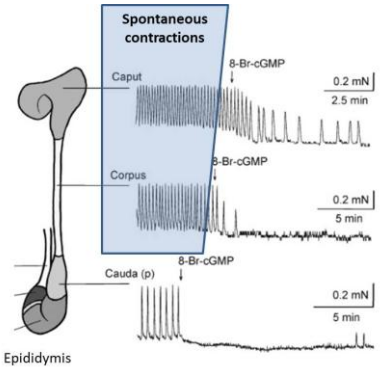

Figure 1-4: Spontaneous contractions of the epididymis without manipulation

Source: Modified after Mewe et al. 2006

Figure 1-4 demonstrates the inhibitory effect of adding 8-Br-cGMP in all three segments. The inhibitory effect on the smooth muscle contraction of the caput is less pronounced in comparison to the other two segments.

Following the removal of the epithelium (Figure 1-5), the number of spontaneous contractions is significantly reduced (Mewe et al. 2006a). The introduction of nora-

drenaline (NE) has been observed to result in an increase frequency of contractions. Following the administration of 8-Br-cGMP, a reduction in frequency was observed (Figure 1-5).

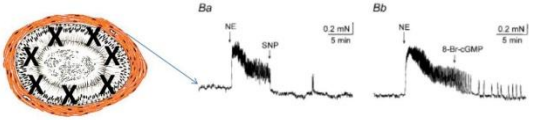

Figure 1-5: Spontaneous contraction following the removal of the epithelium “X”

Source: modified after Mewe et al. 2006a

Additionally, an experiment (Figure 1-6) demonstrated that the removal of all luminal content affects smooth muscle contraction and consequently the cGMP pathway components (Mewe et al. 2006a).

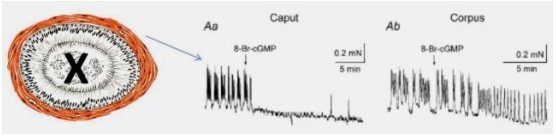

Figure 1-6: Spontaneous contraction in the absence of any lumen content “X”

Source: modified after Mewe et al. 2006b

The aforementioned experiments (Mewe et al. 2006a) and studies on the function of the eNOS (Mewe et al. 2006a) led to the conclusion that epithelial factors must have an effect on smooth muscle contraction (Mewe et al. 2006a; Mewe et al. 2006b; Mietens et al. 2014).

1.1.3 Histology

The ductus epididymidis is covered by a pseudostratified cylindrical epithelium. The main cells in the epididymis, known today as illustrated in Figure 1-7 (Robaire et al. 2015), are:

a) Principal cells which represent 65-80% of the total cells in the epididymis, have a columnar shape with stereocilia on their apical side. They constitute the majority of all epithelial cells throughout the epididymis and are situated on the basal cells (Trasler et al. 1988; Robaire and Hinton 2002; Leung et al. 2004). Principal cells are the primary columnar cells of the epididymis and are responsible for protein secretion and endocytosis. Principal cells contain proton pumps that regulate the acidity of the surrounding environment. At this stage, the spermatozoa require an acidic environment to prevent premature activation and maintain a dormant state during storage in the proximal region (Robaire et al. 2015). In an acidic environment, spermatozoa are unable to move (Welsch

and Deller 2011). Principal cell sub-clusters reflect the anatomical segmentation (Rinaldi et al. 2020).

b) Basal cells (10-20%) are pyramid-shaped cells that sit on the basal lamina. It was believed that they do not reach the lumen. They are present in all segments (Trasler et al. 1988; Robaire and Hinton 2002). However, recent observations have indicated that some basal cells in the epididymal duct also reach the lumen, where they act as luminal sensors (Shum et al. 2008). Basal cells appear to play a pivotal role in maintaining the blood-epididymis barrier, and they may serve as stem cells for the epididymal epithelium (Mandon et al. 2015). It is evident that there are various types of basal cells, yet the precise functions they serve remain uncertain (Rinaldi et al. 2020).

With regard to basal cells, “it is not clear whether all basal cells within taste buds represent a common undifferentiated class of cells. Unambiguous markers for these cells have not been identified, and the exact significance of basal cells as a cell

population remains to be elucidated" (Chaudhari and Roper 2010).

There are 3 times more basal cells in the caput than in the corpus and cauda (Shi et al. 2021).

c) Clear cells (3-10%) are found in the caput, corpus, and cauda. They are responsible for maintaining a physiological pH value (Carr and Acott 1984; Trasler et al. 1988; Shum et al. 2008) through their vacuolar ATPase, which is an ATP-driven proton pump (Shum et al. 2011; Breton and Brown 2013; Robaire et al. 2015). Three distinct subtypes of clear cells have been identified. Two of these cell types are found throughout the epididymis, while the third is found exclusively in the caput and corpus of the epididymis (Rinaldi et al. 2020).

d) Apical cells lack connections to the basement membrane. Their primary function appears to be endocytosis (Robaire and Hinton 2002). They are found in the initial segment (Rinaldi et al. 2020).

e) Narrow cells are present in the initial segment and intermediate zone only (Trasler et al. 1988;

Robaire and Hinton 2002; Cornwall 2009; Robaire et al. 2015).

f) Halo cells (3-10%) may have immunological functions (Trasler et al. 1988; Cornwall 2009; Robaire et al. 2015).

g) Other cells, such as fibroblasts, smooth muscle cells, macrophages, and other immune cells (Bedford 1967; Rinaldi et al. 2020).

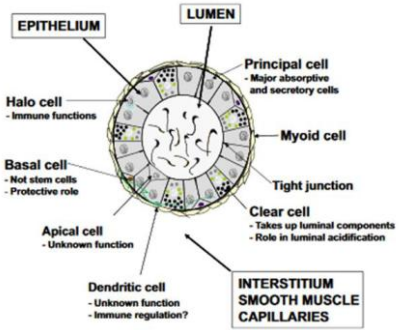

Figure 1-7: Epididymis: main cell types in cross-section observed by light microscopy

Source: Robaire et al. 2015

The epithelium is covered by a layer of smooth muscles that contract spontaneously (Figure 1-4, Figure 3-2) in order to transport the spermatozoa towards the cauda (Mewe et al. 2006a). Following the removal of the epithelium, the number of spontaneous contractions is significantly reduced (Mewe et al. 2006a).

Subsequently, the spermatozoa are transported from the cauda distally to the ductus deferens.

The lumen size and smooth muscle layer thickness increase towards the cauda (Figure 1-8) while epithelium height decreases towards the cauda.

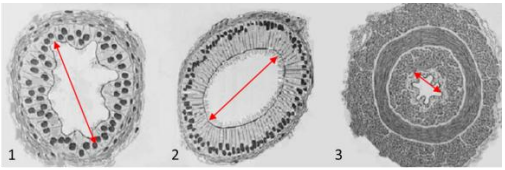

Figure 1-8: Transport path of spermatozoa: comparison of the structures

1: ductus efferentes, 2: ductus epididymidis, 3: ductus deferens

Source: modified after Aumüller and Wurzinger 2010

A study reported the discovery of “a novel phenotype of conjunctival epithelial cells, i.e. a cholinergic cell with chemosensory traits. In analogy to recently described epithelial cholinergic chemosensory cells (CCC) in the thymic medulla, we propose the term “conjunctival CCC” for this entity. A unifying feature of these thymic and conjunctival CCC with cells of similar morphology and phenotype located in respiratory, gastrointestinal, and urethral mucosal surfaces is the expression of components of the canonical bitter and umami taste transduction cascade, such as Gα-gustducin, PLCβ2, and *Trpm5*” (Wiederhold et al. 2015).

1.1.4 T2R signaling cascade

“In mammals, the sense of taste helps in the evaluation and consumption of nutrients and in avoiding toxic substances and indigestible materials. Distinct cell types expressing unique receptors detect each of the five basic tastes: salty, sour, bitter, sweet, and umami. The latter three tastes are detected by two distinct families of G protein-coupled receptors, i.e. T1Rs and T2Rs. Interestingly, these taste receptors have been found in tissues other than the tongue, such as the digestive system, respiratory system, brain, testis, and spermatozoa. The functional implications of taste receptors distributed throughout the body are unknown” (Li 2013). “Although taste receptors for sweet and umami (T1R), bitter (T2R), and salty (ENaC) are known, we know little about their across-species variations, and sour taste and ENaC-independent salt taste are still poorly understood.” (Bachmanov et al. 2014).

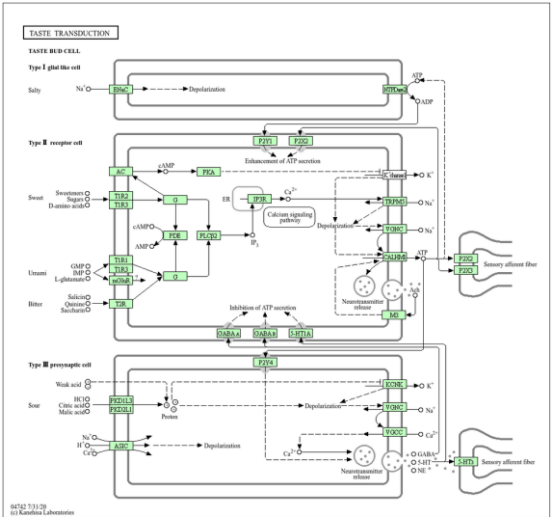

Figure 1-9: Overview of the 5 taste transduction cascades

1) salty, 2) sweet, 3) umami, 4) bitter, 5) sour

Source: Kanehisa et al. 2022
ttps://www.genome.jp/pathway/hsa04742#

The taste transduction pathways are associated with the primary 5 taste characteristics (Figure 1-9). Tas2r receptors are integral to the bitter taste pathway (Kanehisa Laboratory in Kyoto University 2022).

Tas2r108, also referred to as Tas2r8, seems to play a significant role in the lower gastrointestinal tract, facilitating a defensive response (Lu et al. 2017) and a mechanism to eliminate noxious irritants (Kaji et al. 2009)., *Tas2r108* and its downstream signaling molecules, which connect to it, have been identified in the smooth muscle of the mouse gut. These molecules have been demonstrated to react with denatonium benzoate (Avau et al. 2015). The DNT"-induced contraction was further characterized in fundic muscle strips and was shown to be muscle-specific, since blockade of neurotransmission with tetrodotoxin (3 μ M) did not influence the contraction" (Avau et al. 2015).

Figure 1-10 illustrates the interaction of gustducin heterotrimers (alpha-gustducin/Gbeta1/Ggamma13) (Fehr et al. 2007), which are activated by taste cell membranes in the presence of the bitter compound dena-

tonium benzoate (McLaughlin et al. 1993; Huang et al. 1999; Xu et al. 2013).

T2R receptors play a significant role in the defensive mechanism of the trachea. As illustrated in Figure 1-10, motile cilia utilize the T2R transduction pathway to fulfill a mechanical function (Shah et al. 2009).

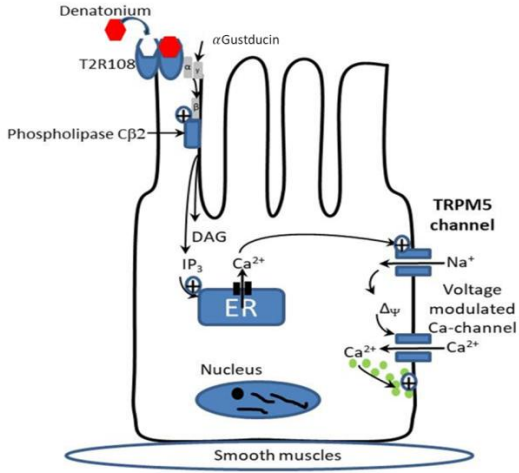

Figure 1-10: *Tas2r108* receptor signaling cascade activated by denatonium

Source: modified after Guinamard et al. 2011

T2R-agonists (e.g., denatonium benzoate) bind at the *Tas2r108* Gq-protein receptors. The α-subunit of the G-protein gustducin serves to activate the phospholipase C (PLC). The βγ-subunit of gustducin is responsible for the hydroxylation of the second messengers inositoltripsphosphate (IP3) and diacylglycerol (DAG) (Liman 2007b). These second messengers facilitate the opening of ion channels within the endoplasmic reticulum (ER), resulting in the release of calcium. This, in turn, activates the Trpm5 cation channel. Subsequently, monovalent ions (e.g., Na^+) can enter the cell, resulting in its depolarization. This depolarization results in opening of voltage-gated ion channels, thereby allowing the influx of extracellular calcium (Liu and Liman 2003). Consequently, choline acetyltransferase (ChAT) facilitates the contraction of smooth muscles through intra- and/or extracellular effects. The latter is not clear yet.

Taste signaling proteins, such as GNAT3 and Trpm5 have been found in the gastrointestinal tract of mice (Bezençon et al. 2007).

Trpm5 has been identified as a taste transducer (Guinamard et al. 2011; Zhang et al. 2003).

1.1.5 Denatonium benzoate

Denatonium (National Center of Biotechnology Information 2020), also known as denatonium benzoate (under various trade names such as BITTER+PLUS, Bitrex, or Aversion), is the most bitter chemical compound known, with bitterness thresholds of 0.05 ppm for the benzoate and 0.01 ppm for the saccharide (US Consumer Product Safety Commission 1992). Its discovery was first reported in 1958 by MacFarlan Smith of Edinburgh, Scotland, during research on local anesthetics. It was subsequently registered under the trademark Bitrex (matthey.com 2017).

Even at concentrations, as low as 10 ppm, denatonium benzoate is unpalatable and perceived as unbearably bitter. Denatonium benzoate is employed as an aversive agent to forestall the inadvertent ingestion of assorted substances, including denatured alcohol, antifreeze, preventive nail biting preparations, respirator mask fit-

testing, liquid soaps, and shampoos (Pulce and Descotes 1996). No long-term health risks have been identified (matthey.com 2017).

Tas2r38 (Meyerhof et al. 2010), a bitter taste receptor in the human body, and *Tas2r108,* a known bitter receptor in mice, react to denatonium benzoate (Avau et al. 2015; Chandrashekar et al. 2000; Bachmanov et al. 2014; Wu et al. 2005).

The effect of denatonium benzoate is transmitted along the G-protein cascade (Figure 1-9, Ogura et al. 1997).

1.1.6 *Trpm5* ion channels

Transient receptor potential (subfamily M melastatin-like, number 5) cation channels (human gene nomenclature 2019) are proteins that connect guanosintriphosphat-binding proteins to a transmembrane receptor in the cell membranes of certain cells (Figure 1-9, Figure 1-10, Clapham et al. 2005, Abramowitz et al. 2007). From an evolutionary standpoint, Trpm5 cation channels represent an ancient gene in yeast. The subfamily of

TRPM channels was designated as such in reference to its inaugural identified member, Melastatin-1 (now designated Trpm1).

The discovery of TRP channels dates back to the 1960s, with the initial publication describing “Clock Mutants of Drosophila melanogaster” (Konopka and Benzer 1971). Subsequent studies have identified the presence of TRP channels in a multitude of organs (Garcia and Schilling 1997). In the mutants of the fly, the photoreceptors responded to light stimuli or depolarization only with a transient, i.e. rapidly inactivating membrane current. In contrast, in the wild type (WT), the current persisted as long as light was incident on the photoreceptor or the depolarization was sustained.

The *Trpm5* receptor is an integral membrane protein comprising six membrane-spanning domains (Liman 2007a; Banik et al. 2018). The N- and C-termini are intracellular. It is a monovalent-specific, non-selective cation channel for ions such as Na^+, K^+, and Cs^+ (Prawitt et al. 2003; Hofmann et al. 2003).

The precise signaling transduction pathway remains uncertain to date. Nevertheless, it is evident that they are voltage-modulated and Ca^{2+}-activated ion channels. They exhibit a response to transient Ca^{2+} changes in concentrations of 0.3-1 µM (Prawitt et al. 2003). Higher concentrations are reported to have an inhibitory effect (Prawitt et al. 2003). *Trpm5* channels have been observed to be active at temperatures between 15°C and 35°C (Talavera et al. 2005).

Trpm5 plays a role in the transduction of taste, mediating the perception of bitter, sweet, and umami (Zhang et al. 2003; Damak et al. 2006; Talavera et al. 2008) as well as fat (Liu et al. 2011).

Dorscht (2020) identified the *Trpm5* protein in the epithelium of the mouse epididymis. Additionally, *Trpm5* has been identified in tuft cells which are also known as brush or brush-cell like cells (Kaske et al. 2007) and other chemosensory cells (Deckmann et al. 2014; Deckmann and Kummer 2016).

In 2017, Carey et al. demonstrated that “product(s) secreted by B. cereus induced NO production and in-

creased ciliary beat frequency (CBF). The response varied markedly between individual patients and involved two important components of bitter taste signaling, phospholipase C isoform β-2 and the transient receptor potential melastatin isoform 5 ion channel (*Trpm5*)."

In other organs, bacteria trigger the gustatory receptor-mediated signaling cascade, which ultimately results in muscle contraction and serves as a protective mechanism (Deckmann and Kummer 2016; Deckmann et al. 2018). In the olfactory system, the absence of *Trpm5* cells with their microvilli has been demonstrated to play an important protective role (Lemons et al. 2017).

A deficiency of *Trpm5* channels may be contributing factor in the development of type 2 diabetes mellitus (Philippaert and Vennekens 2015; Vennekens et al. 2018).

It has been demonstrated that the *Trpm5* cation channel is a critical component of the bitter taste transduction cascade. It has been demonstrated that wild type mice exhibit a response to denatonium benzoate, whereas

Trpm5 KO mice do not react to this substance (Banik et al. 2018).

1.1.7 Clinical relevance

Urinary tract infections (UTI) represent a significant clinical burden, with a high prevalence in urological clinics (Nickel 2019; Wagenlehner et al. 2012; Jhang and Kuo 2017). In most cases, these infections are caused by bacteria and are treated with antibiotics. However, in some cases, these infections can be particularly severe and may necessitate surgical intervention. Epididymitis is characterized by an increase in organ volume and severe pain. In rare cases, benign tumors such as adenocystoma or adenomatoid tumors may be observed (Hoffmann et al. 2000; Schütz and Waldner 2018).

It is evident that the loss of development or malfunction of the initial segment, which consists of segments 1 and 2 in mice, is responsible for infertility as the epididymis plays a pivotal role in sperm maturation (Domeniconi et al. 2016).

It is noteworthy that *Trpm5* cation channels have been identified as a potential contributor to lung cancer (Hantute-Ghesquier et al. 2018).

Nevertheless, the aforementioned diseases of the epididymis have not yet been linked to malfunctions in the *Trpm5* cation channels.

2 Objective of this research

The objective of this research is to compare the contraction characteristics of the smooth muscles of the epididymis between wild type- and *Trpm5 KO* mice. This is done in order to verify the hypothesis that the gustatory signal cascade, specifically the epithelium-specific ion channels, namely the *Trpm5* cation channels, are key for contraction and hence, the defense mechanism of the epididymis.

The null hypothesis is that there will be **no statistically significant** impact of denatonium benzoate on the contraction pattern of the *Trpm5 KO* mice while the alternative hypothesis is expected to show a **statistically significant** variation in the contraction pattern of the smooth muscles of the epididymis of wild type mice. That means that it can be anticipated that no statistically significant results will be observed with regard to the frequency of smooth muscle contractions resulting from the absence of the *Trpm5* cation channel.

Dorscht (2020) demonstrated in her doctoral thesis that a) *Tas2r108* receptors are present in the epididymis

(data not shown) and that b) *Trpm5* ion channels are located in the epithelium but not in the smooth muscle layer (Dorscht 2020; Figure 2-1).

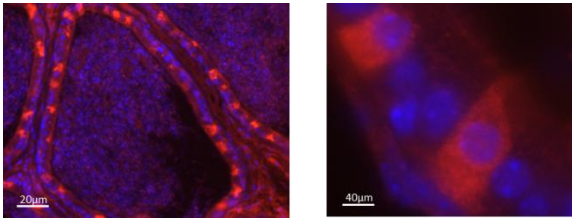

Figure 2-1: *Trpm5* ion channels located in the epithelium of the epididymis

Trpm5 ion channels (red)

Source: Dorscht 2020

The taste receptor *Tas2r108* (Avau et al. 2015; Deckmann et al. 2014; Avau et al. 2015) reacts on ligands such as denatonium benzoate (Chandrashekar et al. 2000; Xu et al. 2013). Cells expressing *Tas2r108*

may contain a *Trpm5* cation channel (Hofmann et al. 2003), which is essential for transducing bitter sensing (Clapp et al. 2001; Pérez et al. 2002; Zhang et al. 2003; Banik et al. 2018).

The initial objective is to identify basal cells that reach the lumen (Shum et al. 2008) through immunohistological techniques using keratin5 as marker for basal cells and in order to confirm the existence of these brush cells or brush-cell like cells (Shum et al. 2008) use Dclk1 as marker for the brush-cells.

The objective is also to confirm coexistence of with basal cells with parts of the signal transduction cascade by using *GNAT3* as marker for the taste proteins.

Secondly, time-lapse imaging, which constitutes the primary component of this study, will investigate whether there are statistically significant differences in the contraction patterns of the epididymal duct when triggered by denatonium benzoate in *Trpm5 KO*- and wild type-mice.

3 Material and methods

3.1 Material

3.1.1 Origin of the research material

For this study, wild type C57BL/6N mice, also referred to as “black 6”, for positive control from the Jackson Laboratory, as well as the transient receptor potential cation channel subfamily M member 5 (*Trpm5*) knockout mice (*Trpm5 KO* mouse), were used. The latter’s genome has a deletion of the 174nt in the area of the 14th exon corresponding to the second transmembrane domain, as well as the introduction of a “Neo-LacZ cassette at the site of the deletion” (Riera et al. 2009).

All animals were housed under standard laboratory conditions and killed by inhalation of an overdose of isoflurane (Abbott) and exsanguination in accordance with § 4 Abs. 3 of the Protection of Animal Act which permits the killing of vertebrates for scientific purposes.

The experiments were approved by the local authorities (Regierungspräsidium) and registered under the following numbers:

- *Trpm5 KO* mouse: 573_M
- *Wild type* mouse (C57BL/6): 571_M

The tissue used in our research was obtained from 15 wild type (15 caput and 13 cauda) wild type and 13 *Trpm5 KO* mice (13 caput and 10 cauda).

The tissues of the epididymis, which were used for the primary experiment, and other organs, which served as controls, were obtained from non-perfused mice.

Following the harvesting of the organs, they were perfused with PFA (4% paraformaldehyde in 0.1 M phosphate buffer at a pH of 7.4) and fixed with Zamboni or Bouin, then post-fixed overnight.

Some organs were promptly frozen (without fixation) in liquid nitrogen for RT-PCR or cryostat cutting.

The remaining organs were maintained in minimal essential medium (MEM; Gibco, Invitrogen, Karlsruhe,

Germany) at 4°C until preparation within the subsequent one to two hours.

3.1.2 Software, equipment, consumables, solutions, kits

Table 3-1: Software

Name, Version	Producer
ImageJ 1.5x/ Fiji	http://imagej.net/
Motic Images Plus 2.0	Motic Germany GmbH, Wetzlar
Motic Images Plus 3.0	Motic Germany GmbH, Wetzlar
GraphPad Prism 10.2	GraphPad Software, Inc., La Jolla
Axiov. Rel 4.8	Zeiss, München

Source: Own compilation

Table 3-2: Equipment

Product	**Producer**
Agarose Gel Electrophoresis Chamber	PeqLab, Erlangen
Culture Dish Micro-Observation Temperature Control System- and dish warmer T5NODR (8251-12-09)	Biotechs, California
Fluorescent microscope, Axioskop 2plus	Zeiss, München
Gel-Documentation system	Phase, Lübeck
Kryostat, CM1900	Leica, Wetzlar
Leica microscope MS5	Leica, Wetzlar
MasterCycler Gradient	Eppendorf, Hamburg
Nanodrop 2000 Spectrophometer	Thermo Scientific, Waltham, USA
Motic microscope	Motic Germany GmbH, Wetzlar
MoticCam 3.0 MP+	Motic Germany GmbH, Wetzlar

MoticCam 3.0 MP	Motic Germany GmbH, Wetzlar
Motic Bi-okkular SMZ-171	Motic Germany GmbH, Wetzlar

Source: Own compilation

Table 3-3: Consumables

Product	**Producer**
Cover glasses	Langenbrick, Emmendingen
Delta T Dish	Biotechs, California
Eppendorf Tubes (0,5ml/1,5ml/2ml)	Eppendorf, Hamburg
Pipette tips (2,5/10/20/100/1000µl)	Eppendorf, Hamburg
Superfrost® Plus object holder	R. Langenbrinck, Emmendingen

Source: Own compilation

Table 3-4: Solutions

Solution	**Producer**
I-Chloro-2,2,2Trifluoroethl-Difluoromethylether (Isofluran)	Abbott, Wiesbaden
4‘6-diamidino-2-Phenylindol (DAPI)	Sigma-Aldrich, Steinheim
β-Mercaptoethanol	Sigma-Aldrich, Steinheim
Agarose	PeqLab, Erlangen
Bovine serum albumin (BSA)	Sigma-Aldrich, Steinheim
DMEM/F-12 (1:1)	Gibco®, Invitrogen, Grand Island, USA
Denatonium benzoate	Molecula GmbH, München
Acetic acid	Merck, Darmstadt
Ethanol	Riedel de Haen, Seelze
Ethidium bromide	Roth, Karlsruhe
Formaldehyde solution	Roth, Karlsruhe
Glycerol	Roth, Karlsruhe
Hepes	Sigma-Aldrich, Stein-

	heim
Isopropanol	Sigma-Aldrich, Steinheim
Methanol	Fluka, Buchs, Switzerland
Minimum Essential Medium (MEM)	Gibco® by life technologies™, Grand, USA
Natriumazid (NaN_3)	Sigma-Aldrich, Steinheim
Natrium-Chlorid (NaCl)	Roth, Karlsruhe
di-Natriumhydrogenphosphat-Dihydrat (Na_2HPO_4)	Roth, Karlsruhe
Natriumdihydrogenphosphat-Monohydrat (NaH_2PO_4)	Merck, Darmstadt
Sodium hydroxide (NaOH)	Merck, Darmstadt
Noradrenaline (Norepinephrin)	Sigma-Aldrich, Steinheim
Normal horse serum	Abcam plc, Cambridge
Normal goat serum	Sigma-Aldrich, Steinheim
Orang-G	Sigma-Aldrich, Steinheim

Paraformaldehyd	Roth, Karlsruhe
Picric acid	Fluka, Buchs
Saccharose	Roth, Karlsruhe
Tissue-Tek O.C.T.	Sakura, Zoeterwoude, Netherlands
Tris	Roth, Karlsruhe
Xylol	Roth, Karlsruhe

Source: Own compilation

3.2 Methods

3.2.1 Immunostaining

For immunostaining, PFA and Zamboni fixed organs were washed overnight in 0.1 M phosphate buffer and run consecutively through a series of different sugar solutions (10%, 20%, 40% sucrose – each one separately overnight) before freezing in nitrogen by using 2-methylbutan. Additionally, Bouin-fixed tissues were paraffin-embedded. For immunofluorescence staining of cryo tissues, frozen specimens were cut into 10 µm sections and transferred to slides. The sections were then allowed to dry at room temperature. Paraffin-embedded tissues were sectioned at a thickness of 5 µm using the RM Leica 225, transferred to slides, and subsequently air-dried at 40°C in an incubator overnight. Following deparaffinization (xylol 3x5 minutes, ethanol (100%, 96%, 70%), aqua dest., PBS each 5 minutes), all sections (same protocol for paraffin and cryo) were washed in PBS and for blocking of unspecific protein binding sites treated with 2% normal horse (or normal

goat subject to the primary antibody) serum for 1h at room temperature.

Subsequently, the specimens were incubated with primary antibodies (see table 3.2.1.1.1) overnight at 4°C in a humid chamber.

The control samples were not incubated with primary antibodies.

Subsequently, the slides were washed with PBS (2x10min.), stained with secondary antibodies (see table 3.2.1.1.2), and 4'6-diamidino-2-phenyl-indole (DAPI) at room temperature for 1h in the dark. Finally, the cells were washed (2x10 min.) with PBS, followed by fixation with PFA and washed again (2x10 min.).

All incubations were conducted in a "humid chamber".

Subsequently, the cuts were sealed with PBS+Glycerol (1:3) and stored at 4°C.

Images were captured using the Zeiss Axioskop 2 Plus microscope.

The protocol can be found in the appendix on page 138 (Figure 8-1).

3.2.1.1 Antibodies

3.2.1.1.1 Primary antibodies of the immunostaining

Table 3-5: Primary antibodies used for immunohistochemistry

Antigen	Abrev.	Supplier	Source	Dilution	Function
Cytokeratin 5	Keratin5	Spring Bioscience (Pleasanton, USA)	Rabbit	1:200	Basal cell marker
Cytokeratin 5	Keratin5	Spring Bioscience (Pleasanton, USA)	Chicken	1:400	Basal cell marker
Cy-	COX-1	Ca-	Rabbit	1:200	Mark-

cloox-ygen-ase 1		yman Che-mical (Ann Arbor, MI, USA)			er for basal cells (Leun g et al. 2004)
Gua-nine nucle-otide-bind-ing protein G(t) subu-nit alpha-3, also gustdu cin alpha-3 chain	GNAT 3	Coava lab	Goat	1:800	Enter-oendo do-crine cells, immu-nore-activity (rat duode de-num), taste cell related mark-er (Suth-erland et al. 2007; Höfer et al. 1996)
Double ble-cortin like	Dclk1	abcam (Cam-bridge, Eng-	Rab bit	1:1000	Enter-oendo do-crine

kinase 1		land)			cells, high-lights micro-tubule (Gerbe et al. 2011)

3.2.1.1.2 Secondary antibodies of the Immunostaining

Table 3-6: Secondary antibodies used for immunohistochemistry

Name	Supplier	Dilution in PBS
Alexa, 488 Goat-anti-Rabbit-IgG	Life technologies-Invitrogen (Darmstadt, Germany)	1:400
Alexa, 546 Donkey-anti-Goat-IgG	Life technologies-Invitrogen (Darmstadt, Germany)	1:400
Alexa, Cy3 Goat-anti-Rabbit-IgG	Life technologies-Invitrogen (Darmstadt, Germany)	1:400
Cy311 Donkey-anti-Rabbit-IgG	Merck Millipore (Schwalbach, Germany)	1:400

FITC Donkey-anti-Chicken-IgG	Jackson Immuno Research (Dianova) (Hamburg, Germany)	1:800

Sources: All tables in section 3 have been compiled by Haas

3.2.2 Time-lapse imaging

In order to visualize the contraction of the epididymal duct, parts of the epididymal duct of the wild type and *Trpm5 KO* mouse were isolated by careful dissection under direct observation with a binocular microscope. Comparable segments were excised from the caput (segment 2) and cauda (segment 8) of the epididymal duct (Figure 3-1) from the tissue of each of the two mouse types. This signifies that a series of 4 distinct experiments was conducted.

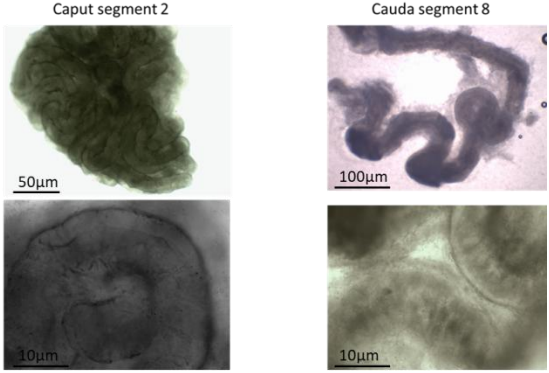

Figure 3-1: Mouse epididymis caput and cauda in different magnifications

A collagen stock solution was prepared using collagen fibers isolated from four rat tails, which were conserved at -20°C. The rat tails were allowed to thaw in a solution of 70% ethanol, after which connective tissue was removed. The collagen fibers were extracted from the tissue and soaked in 70% ethanol for 15 to 20 minutes. After drying, fibers were agitated at 4°C in 250 ml of 0.1% acetic acid for 48 hours. The resulting viscous collagen suspension was subjected to centrifugation at 4°C at 24,000 rpm under sterile conditions. The transparent supernatant was subsequently stored at 4°C.

One gram of collagen was combined with 150 ml of 106DMEM/ F12 (Gibco, Invitrogen, Karlsruhe, Germany), 30 ml glacial acetic acid, 42 ml 0.5 M NaOH and 22.5 ml HEPES with vortexing after the addition of each component. Upon the addition of NaOH, the solution undergoes a color change from pale yellow to pink and then back to yellow upon the addition of HEPES.

Immediately upon pipetting at the bottom of the microscopy dish, the collagen began to undergo polymerization.

The epididymal duct segment of each mouse was positioned in the center of the solution, and care was taken to ensure that the duct segment was fully covered with the collagen to prevent desiccation.

Following a 30 minutes polymerization period at 37°C in an incubator, the dishes were covered with 1 ml of MEM to protect the samples and prevent tissue deterioration.

Just prior to commencing data acquisition, 330 µl MEM was added to maintain liquid balance within the dish throughout the experiment.

The dishes containing the epididymal duct segments were maintained at 34°C with images captured at one-second intervals.

The duct segment was monitored under transmitted light with a magnification of 25 using a Motic microscope with the Motic Cam 3.0.

The movies were analyzed using ImageJ 1.5x (public domain software, NIH, USA, downloadable at http://rsb.info.nih.gov/ij).

Spontaneous muscle contractions were recorded in four phases; 1) no treatment (spontaneous contraction), 2) and 3) addition of denatonium benzoate (DNT), a bitter compound, at two different concentrations, 10 µM and 100 µM, respectively. In the final phase, noradrenaline was administered to assess the viability of the tissue.

The duration of the treatment period was 8 min for each of the 4 phases.

To facilitate visualization of the contractions, time-lapse images were captured at a rate of one frame per second by creating a virtual section through the wall of the epididymal duct.

When necessary, contrast enhancement was employed for enhanced visualization of minor peaks. The twitches were enumerated within a defined time frame of 300 seconds to ascertain the frequency of contractions, ensuring comparability. Counting started 60 seconds after the application.

Isolated segments of the epididymal duct from a wild type mouse (caput) and *Trpm5 KO* mouse (cauda) are

used for time lapse imaging (Figure 3-1, Figure 4-4, Figure 4-5).

Figure 3-2A provides a representative snapshot of the movie, which depicts the caput segment 2 of the epididymal duct of wild type mouse. Figure 3-2B shows the time stack, a series of images captured over time, in a movie of the caput of a *Trpm5 KO* mouse.

The reslices (Figure 3-2A and B), which represent the visual contractility derived from virtual sections through the corresponding time stacks at the outset (“no treatment”) and following each treatment with 10 µM and 100 µM denatonium benzoate for the respective duct segment, comprise the basis for the statistical analysis. These reslices reflect the spontaneous muscle contraction and the effects of the treatments.

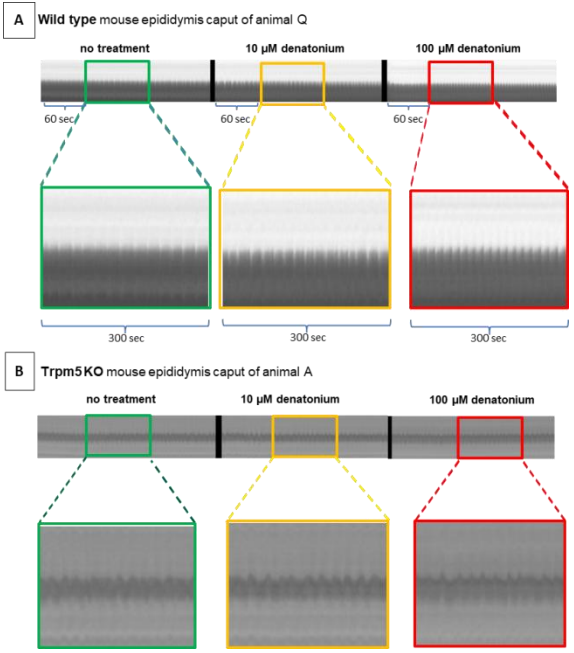

Figure 3-2: Example of time-lapse imaging

Raw data of caput and cauda for WT and Trpm5 KO mice epididymis is provided in the appendix (page 140).

The application of drugs is indicated by the colored frames (Figure 3-2A and B) illustrate the effects of substances in question. The small peaks observed at the reslice (Figure 3-2A and B) represent muscle contractions.

As observed in the wild type mouse, the frequency of contraction increased in this example, whereas the *Trpm5 KO* tissue appeared unaltered following the application of denatonium benzoate.

For purposes of enhanced visual clarity, the illustration does not depict the contractility resulting from noradrenaline donation. This was solely a confirmation of the tissue's vitality at the end of each experiment.

3.2.2.1 Statistical analysis

3.2.2.1.1 Data capturing and basic calculations

The data for the time-lapse imaging was captured in Microsoft Excel spreadsheets, which are attached in section 8.6 of the appendix for reference (Table 8-1, Table 8-2).

3.2.2.1.2 Statistical methods

A **repeated measures (RM) one-way ANOVA** (Ostertagova and Ostertag 2013) was performed using GraphPad Prism software for the statistical analysis. A one-way ANOVA hypothesis test follows a step-wise procedure by first stating the null hypothesis H0 and alternative hypothesis, then in step 2 decides on the significance level, α which is α = 0.05 followed by step 3 computing the p-value.

The experimental design was constructed in a manner that allows for the assumption of a Gaussian distribution of the date represented in each row. With regard to the issue of sphericity, the Geisser-Greenhouse correction was selected in accordance with the recommendation set forth in the literature (GraphPad 2023).

A repeated-measures ANOVA was employed to compare the mean of each column with the mean of every other column.

To compute the P value, which represents the level of significance, the Tukey test (Lee and Lee 2018; GraphPad 2020) was employed as the multiple compar-

isons test and the “correct for multiple comparisons using statistical hypothesis testing” option was selected, as recommended. The option was selected to report a multiplicity-adjusted P value for each comparison. Each P-value is adjusted to account for multiple comparisons. A 95% confidence interval was selected. If the Tukey test does not cross the 0, the result is statistically significant. GraphPad reports a q-value to compare Prism's results with texts or other statistical programs. Note that this use of the variable q is distinct from the use of q when using the FDR approach.

Additionally, the F-value, which is the ratio between the variance within groups and the variance between groups, is displayed. A high F-value indicates that the variance between groups is greater than the variance within groups. This indicates that there is a statistically significant difference between the group means.

The Tukey test is similar to the t-test, but has the special property that it keeps the error level constant at around 5%. With the t-test, the probability of error would be beyond 40%. As mentioned above, the t-test is not

possible as this experiment consists of more than two random samples.

The data were subjected to a normality test, namely the “omnibus K2” D’Agostino & Pearson test, which is a versatile and powerful tool for this purpose (D'Agostino 1973). Moreover, normality was assessed using the Anderson-Darling, the Shapiro-Wilk and the Kolmogorov-Smirnov tests (GraphPad 2020).

Outliers were identified using the ROUT method at both the 1% and 10%, levels. ROUT set at 1% would be sufficient. However, to be more conservative, ROUT was set to 10%.

The statistical analysis was discussed and agreed upon with the working group “Stochastics” of the Mathematical Institute at Justus-Liebig-University, Gießen.

The results are presented in section 4.2.1 “Repeated-measures one-way ANOVA” at a glance.

The underlying data are presented in the appendix (page 140). Statistical terms are explained in the appendix (page 148).

4 Results

Based on the objective of this research, the results are based on two pillars to characterize and compare the contractile patterns of the smooth muscle of the epididymis of wild type and Trpm5 KO mice:

First (4.1 Immunohistology), immunohistological studies of mouse epididymis have been performed to detect and analyze basal cells and its subpopulation with slender processes towards the lumen. Keratin5 antibodies were used to visualize these basal cells. GNAT3 antibodies were used to detect proteins of the taste transduction cascade and Dclk1 antibodies as marker for tuft cells.

Second (4.2 Time-lapse: Impact of Trpm5 ion channel on DNT induced contraction), after application of denatonium benzoate it is hypothesized that there will be a statistically significant difference in the contractile pattern of the smooth muscle of the epididymis of wild type mice, whereas there will be no statistically significant effect of the contractile pattern of the Trpm5 KO mice.

4.1 Immunohistology

4.1.1 Basal cells and their subpopulation with cytoplasmic slender processes

To search for keratin5-positive basal cells with slender processes towards the lumen, segments 2 (caput) and 8 (cauda) of the paraffin-embedded tissue of the epididymis of wild type mice were analyzed.

In caput of segment 2 (Figure 4-1) shows segment 2 of wild type mouse epididymis stained with keratin5. The majority of cells represent basal cells with a wide body at the basal membrane. Also, there are several cells with similar shape but slender processes towards the lumen, i.e. a subpopulation of basal cells. The number of these cells is much smaller than the number of regular basal cells. In very few cases the slender process of this subpopulation reaches the lumen (Figure 4-3A; arrowhead ➢).

The dashed line serves to visualize the transition from epithelium to lumen.

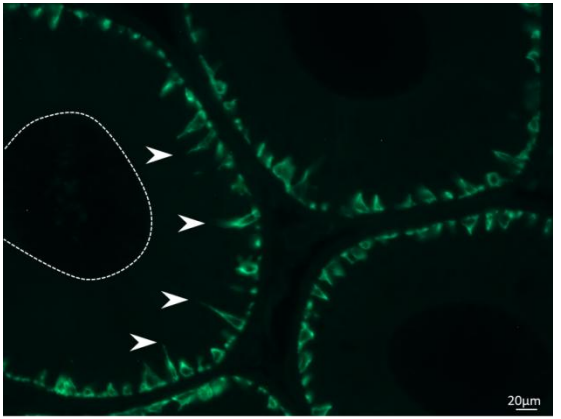

Figure 4-1: Wild type mouse epididymis caput basal cells immunostaining keratin5 with a subpopulation of basal cells with slender processes (arrowhead ➤) towards the lumen (--- dashed line)

4.1.2 Co-expression of basal cell and taste transduction markers

In a next step, double staining of a paraffin-embedded wild type mouse epididymis caput with keratin5 and GNAT3 confirms the presence of basal cells in the caput

that are reaching towards the lumen (Figure 4-1 and Figure 4-2A; **green**).

There are also a few cells which are GNAT3 positive, i.e. contain proteins of the taste transduction cascade (Figure 4-2B; **red**). As outlined above, the taste transduction cascade also contains a Trpm5 cation channel, which seems to be responsible for the contraction of the smooth muscles of the epididymal duct (see Figure 1-10).

Finally, a co-expression of both antibodies, keratin5 and GNAT3, could be found in wild type mice epididymis (Figure 4-2C). This demonstrates the co-existence of the taste transduction cascade in keratin5-positive basal cells and thus the relationship to smooth muscle contraction.

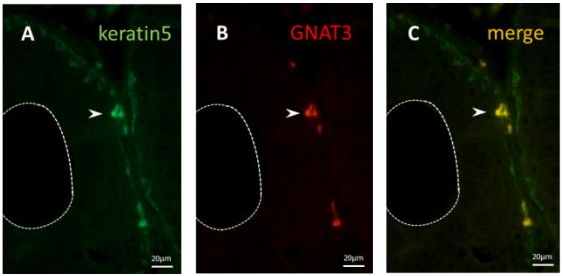

Figure 4-2: Double staining of WT ms epididymis with antibodies against keratin5 (green) and GNAT3 (red) and co-expression of keratin5 and GNAT3 (merge) of a subpopulation of basal cells with slender processes (arrowhead ➢) towards the lumen (---dashed line)

4.1.3 Co-expression of basal cell and tuft cell markers

Double staining of a paraffin-embedded wild type mouse epididymis with keratin5 (Figure 4-3A, **green**) confirmed the characterization as a subpopulation of basal cells with a wide basis and an apical slender process into the lumen (arrowhead ➤), and Dclk1 (Figure 4-3B, **red**) as marker for tuft cells in keratin5-positive basal cells, i.e. represents the chemosensory function of the cells.

The co-expression of both antibodies can be visualized (Figure 4-3C).

This is a proof that the subpopulations of basal cells which contain chemosensory function reach the lumen of the epididymal duct in order to protect the organism against UTI.

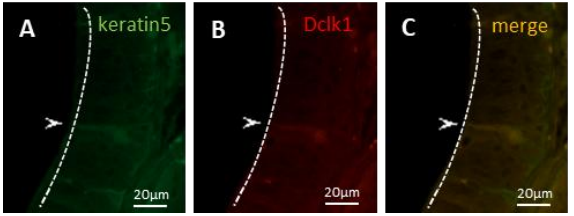

Figure 4-3: Double staining of WT ms epididymis with antibodies against keratin5 (green) and Dclk1 (red) and co-expression of keratin5 and Dclk1 (merge) of a subpopulation of basal cells with slender processes (arrowhead ➢) reaching the lumen (---dashed line).

4.2 Time-lapse: Impact of Trpm5 ion channel on DNT induced contraction

The dissected tissue (caput – segment 2 and cauda segment 8) of the epididymis of wild type and Trpm5 KO mice (Figure 4-4, Figure 4-5) was used to measure and analyze statistical significances in regard to smooth muscle contraction for both types of mice. The wild type mice contain a Trpm5 cation channel whereas the Trpm5 KO mice do not contain the Trpm5 cation channel.

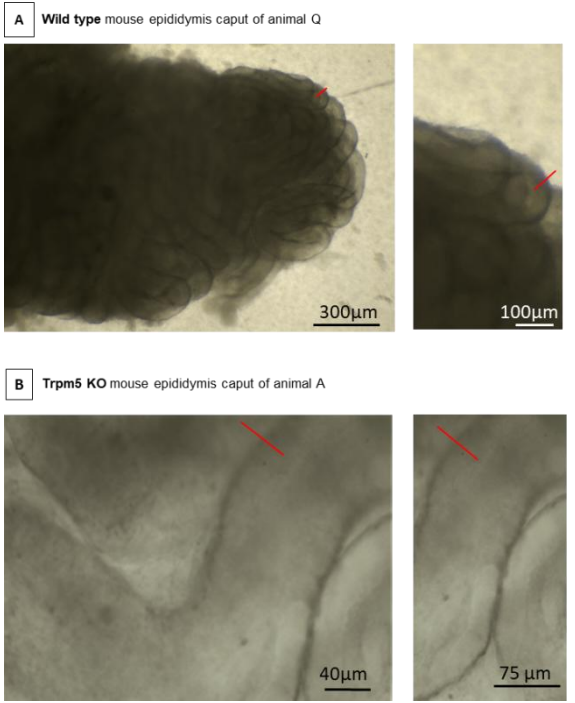

Figure 4-4: WT and Trpm5 epididymis caput snapshots
Dissected tissue of mouse epididymis segment 2 of caput for A wild type and B Trpm5 KO mouse. The red line marks the region of the tissue where the contraction was registered for the reslices (see Figure 4-6)

This study comprises 4 time-lapse experiments as outlined in section 3.2.2 with the objective of evaluating or confirming the hypothesis presented in section 2.

In order to visualize the contraction of the epididymal duct, parts of the epididymal duct of the wild type and *Trpm5 KO* mouse were isolated by careful dissection under direct observation with a binocular microscope. Comparable segments (Figure 4-4A and B, Figure 4-5A and B) were excised from the caput (segment 2) and cauda (segment 8) of the epididymal duct from the tissue of each of the two mouse types. A series of 4 distinct time-lapse experiments was conducted:

1) Wild type caput and 2) Trpm5 KO caput (Figure 4-6),

3) Wild type cauda and 4) Trpm5 KO cauda (Figure 4-7).

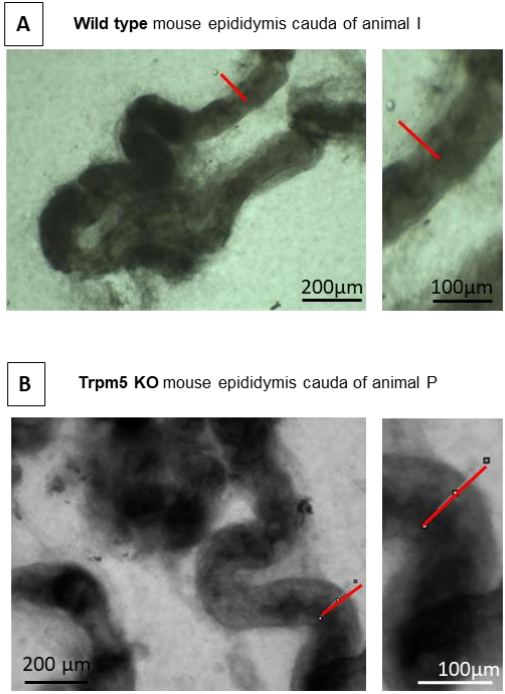

Figure 4-5: WT and Trpm5 epididymis cauda snapshots

Dissected tissue of mouse epididymis segment 8 of cauda for wild type (A) and Trpm5 KO mouse (B). The red line marks the region of the tissue where the contraction was registered for the reslices (see Figure 4-7)

60 photos per minute were taken (Figure 4-6A and B, Figure 4-7A and B), using a Motic microscope with the Motic Cam 3.0, and analyzed using ImageJ 1.5x (public domain software, NIH, USA, downloadable at http://rsb.info.nih.gov/ij) over a period of 8 minutes for each of the 4 phases generating a reslice (Figure 4-6A and B as well as Figure 4-7A):

1) spontaneous contraction without any treatment, 2) application of denatonium benzoate (DNT) 10 µM, 3) application of denatonium benzoate (DNT) 100, 4) application of noradrenaline to assess the viability of the tissue (not shown in the reslice) (Figure 4-6A and B, Figure 4-7A and B).

The twitches were enumerated within a defined time frame of 300 seconds, start counting 60 seconds after the application, to ascertain the frequency of contractions and ensuring comparability (Figure 4-6A and B, Figure 4-7A and B). The amplitude remained unchanged within each of the four experiments.

However, as for wild type mice epididymis caput and cauda a change in frequency could be observed (Figure

4-6A, Figure 4-7A) from a stable spontaneous contraction pattern to a higher frequency after the application of DNT (10µM and 100µM).

In Trpm5 KO epididymis caput and cauda, the frequency remained stable throughout the entire experiment (Figure 4-6B, Figure 4-7B), from spontaneous contraction to the application of 10µM DNT and 100µM DNT, respectively.

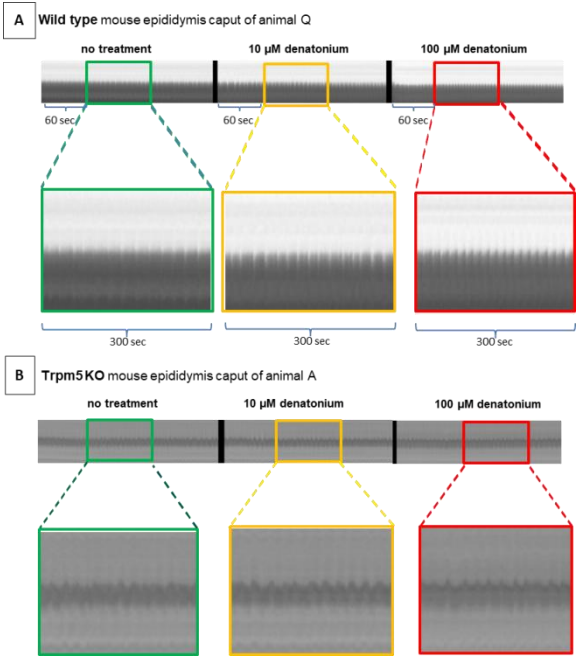

Figure 4-6: Time-lapse imaging WT and Trpm5 epididymis caput

Reslice of mouse epididymis segment 2 of caput of wild type (A) and Trpm5 KO mouse (B). The image sections show the recording 60seconds after start of the experiment and 60 seconds after each application: No treatment (spontaneous contraction, green frame), after

application of 10µM (yellow frame) and 100µM (red frame) denatonium.

A visual assessment of the resliced data, devoid of any scientific rigor, reveals a striking consistency in contraction patterns throughout the entire experiment (Figure 4-6B, Figure 4-7B) for Trpm5 KO caput as well as cauda. As outlined in the summary of Table 4-8, the statistical result is “ns” (no significance) for both the Trpm5 caput and the Trpm5 cauda. This confirms the visual impression noted here.

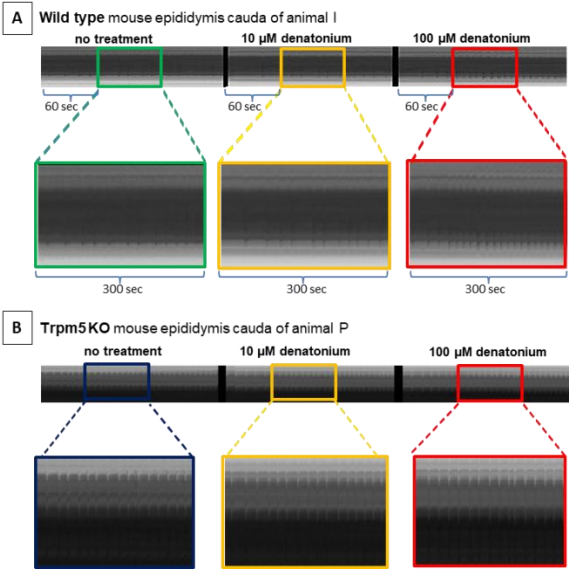

Figure 4-7: Time-lapse imaging WT and Trpm5 epididymis cauda

Reslice of mouse epididymis segment 8 of cauda of wild type (A) and Trpm5 KO mouse (B). The image sections show the recording 60seconds after start of the experiment and 60 seconds after each application: No treatment (spontaneous contraction, green frame), after application of 10µM (yellow frame) and 100µM (red frame) denatonium.

As for the WT mice epididymis caput and cauda, the reslice (Figure 4-6A, Figure 4-7A) demonstrates the increase in contraction frequency. Finally, after data collection, a repeated-measures (RM) one-way analysis of variance (ANOVA) was employed to statistically assess the null hypothesis that the Trpm5 cation channel plays a significant role in the contraction of the epididymal duct of the mouse (4.2.1 “Repeated-measures one-way ANOVA) and hence, **no statistical significant** results for the Trpm5 KO mice caput and cauda (Table 4-9). **Statistical significant** results could be expected for the wild type mice epididymis contraction patterns for caput and cauda (Table 4-9) in order to confirm the aforementioned alternative hypothesis.

4.2.1 "Repeated-measures one-way ANOVA" at a glance

As this experiment consists of more than two random samples, repeated-measures (RM) one-way ANOVA (Ostertagova and Ostertag 2013) had to be conducted in order to compute the p-values for the 4 time-lapse experiments. The significance level α was set to α=0.05 as usual for similar scientific research projects.

Data was normal distributed (Table 8-3, Figure 4-8D, Figure 4-9D, Figure 4-10D, Figure 4-11D).

There were no outliers (Table 4-5).

The matching for all 4 experiments is effective demonstrating significant match (Table 4-7).

Statistically significant results (Table 4-8,Table 4-9) could be observed for wild type mouse epididymis caput (Figure 4-8) and cauda (Figure 4-9) as shown in the graphical summaries below. There **were no statistically significant** results (Table 4-8,Table 4-9) for Trpm5

KO mice in either caput (Figure 4-10) or cauda (Figure 4-11).

Explanations of the statistical terms are provided in the supplement (page 148 Explanation of the statistical terms).

4.2.1.1 RM one-way ANOVA for WT mouse epididymis caput

The one-way ANOVA for WT mouse epididymis caput showed a **significant** effect of DNT on the frequency of smooth muscle contraction: $F(1.578, 22.09) = 9.985$, $p < 0.05$ (Table 8-4).

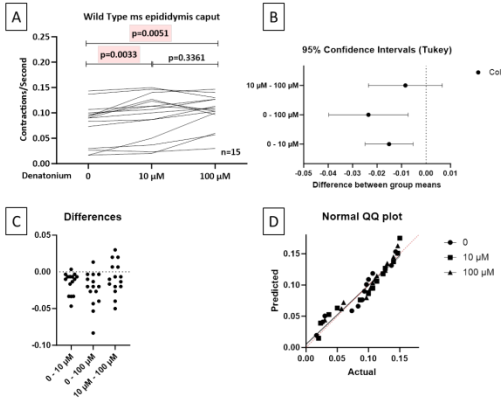

Figure 4-8: Wild type mouse epididymis caput - graphs

In further detail, the RM one-way ANOVA results for the caput of the wild type mice (Table 4-9; Figure 4-8A, Table 4-1) revealed statistically **significant** differences between the 'no treatment' (spontaneous contraction) and the treatment phases. The application of '10 µM DNT' yielded in a p-value of 0.0033, while the comparison between the 'no treatment' and '100 µM DNT' phases yielded in a p-value of 0.0051.

The comparison under the 95% confidence interval (Tukey) between the 10 µM DNT and 100 µM DNT did **not** yield a **statistically significant** difference

(p = 0.3361). However, the Tukey test is only 0.00663 above 0 (numbers not shown, Figure 4-8B, Table 4-1). The differences plot (Figure 4-8C) shows a wider range as expected compared to the Trpm5 KO mice.

The QQ plot confirms homoscedasticity, i.e. it shows that the scatter of the points around the straight line in the vertical direction is constant. The simultaneous display of both lines indicates that both the predictive relationship between the variables (auxiliary line - red) and the strength and direction of the correlation (correlation line - black) are emphasized in the graph. As both lines are very similar, it supports the assumption of a strong linear relationship. That indicates a normal distribution as computed with the normal distribution tests (Figure 4-8D, Table 8-3).

In summary of the first set of experiments of WT epididymis caput the statistical analysis resulted in the following data sets (Table 4-1):

Table 4-1: Tukey's multiple comparison test: WT mouse epididymis caput

Repeated measures one-way ANOVA - Multi comparisons
WT ms epididymis caput - Data

Input

Number of families	1
Number of comparisons per family	3
Alpha	0,05

Output

Tukey's multiple comparisons test	Mean Diff,	95,00% CI of diff,	Below threshold?	Summary	Adjusted P Value	
0 vs. 10 µM	-0,0151	-0,02493 to -0,005295	Yes	**	0,0033	A-B
0 vs. 100 µM	-0,0236	-0,03977 to -0,007353	Yes	**	0,0051	A-C
10 µM vs. 100 µM	-0,0084	-0,02353 to 0,006633	No	ns	0,3361	B-C

Test details	Mean 1	Mean 2	Mean Diff,	SE of diff,	n1	n2	q	DF
0 vs. 10 µM	0,0798	0,0949	-0,0151	0,0038	15	15	5,6970	14
0 vs. 100 µM	0,0798	0,1033	-0,0236	0,0062	15	15	5,3810	14
10 µM vs. 100 µM	0,0949	0,1033	-0,0084	0,0058	15	15	2,0730	14

Input: The “number of families” equals the WT mouse caput (=1), the number of comparisons contains the 3 different levels of measurement (spontaneous contraction, 10µM and 100µM DNT application), alpha was set at a p-value benchmark at α = 0,05.

Output: The Tukey’s multi comparison test shows the results of the RM one-way ANOVA for the 3 different phases of the experiment, namely O (spontaneous contraction) vs. 10µM DNT (adjusted p-value p=0.0033) and vs. 100µM DNT (p=0.0051) respectively as well as 10µM vs. 100µM DNT (p=0.3361).

Also, the statistical test details (“mean difference”, 95% confidence interval of difference, if the result is below the threshold (i.e. 0,05), a statistical summary (with * highlighting statistical significance), the label of the effects (A = no treatment, B = 10µM DNT, C = 100µM DNT), mean1 and 2, difference of means, SE (standard error) of difference between the means, n1 and n2 (the number of subjects, i.e. mice), q and DF (degree of freedom = the number of subjects-1) are provided for the computation of the RM one-way ANOVA with a q-value to compare it with other statistical computations.

It is evident that the caput can already be stimulated by a low dose of DNT without any further effects being observed at higher concentrations (i.e., 'no treatment' vs. 10 µM DNT). However, between 10µM and 100µM the effect is statistically not significant.

4.2.1.2 RM one-way ANOVA for WT mouse epididymis cauda

The one-way ANOVA for WT mouse epididymis cauda showed a **significant** effect of DNT on the frequency of smooth muscle contraction: $F(1.702, 20.43) = 8.069$, $p < 0.05$ (Table 8-5).

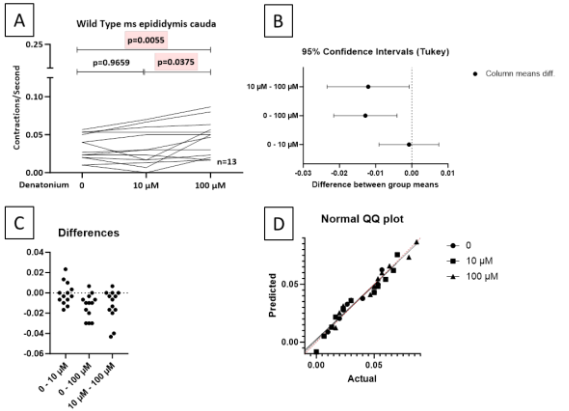

Figure 4-9: Wild type mouse epididymis cauda - graphs

With regard to the cauda of the wild type mice epididymis (Table 4-9 and Figure 4-9A, Table 4-2), the results are as follows: "**No significant**" difference was observed between the 'no treatment and 10 µM DNT phases (p = 0.9659).

With regard to the cauda, a "**significant**" difference was observed in the following cases: The comparison between the 'no treatment' and '100 µM DNT' yielded a p-value of 0.0055, while the comparison between the '10

µM DNT' and the '100 µM DNT' phases yielded in a p-value of 0.0375.

This suggests that the cauda may require a higher dose of DNT to increase its frequency compared to the caput.

Being within the 95% confidence interval, the auxiliary and the correlation lines are very similar confirming the normal distribution of data (Figure 4-9D, Figure 4 7, Figure 4 8, Table 8 3).

The differences plot (Figure 4-9C) and 95% confidence intervals (Tukey) show results which are expected with the wild type mice epididymis caput and comparable to the WT mice caput.

Table 4-2: Tukey's multiple comparison test: WT mouse epididymis cauda

Repeated measures one-way ANOVA - Multi comparisons
WT ms epididymis cauda- Data

Input

Number of families	1
Number of comparisons per family	3
Alpha	0,05

Output

Tukey's multiple comparisons test	Mean Diff,	95,00% CI of diff,	Below threshold?	Summary	Adjusted P Value	
0 vs. 10 µM	-0,0008	-0,009022 to 0,007465	No	ns	0,9659	A-B
0 vs. 100 µM	-0,0128	-0,02159 to -0,004068	Yes	**	0,0055	A-C
10 µM vs. 100 µM	-0,0121	-0,02342 to -0,000690	Yes	*	0,0375	B-C

Test details	Mean 1	Mean 2	Mean Diff,	SE of diff,	n1	n2	q	DF
0 vs. 10 µM	0,0328	0,0336	-0,0008	0,0031	13	13	0,3555	12
0 vs. 100 µM	0,0328	0,0457	-0,0128	0,0033	13	13	5,5250	12
10 µM vs. 100 µM	0,0336	0,0457	-0,0121	0,0043	13	13	4,0020	12

The Tukey tests for the wild type mice caput and cauda (Figure 4-8B, Figure 4-9B, Table 4-1, Table 4-2,Table 8-3) illustrate the statistically significant results for the wild type mice epididymis caput and cauda thus confirming the alternative hypothesis.

4.2.1.3 RM one-way ANOVA for Trpm5 KO mouse epididymis caput

The one-way ANOVA for Trpm5 KO mouse epididymis caput showed **no significant** effect of DNT on the frequency of smooth muscle contraction: F (1.368, 16.42) = 1.405, p > 0.05 (Table 8-6).

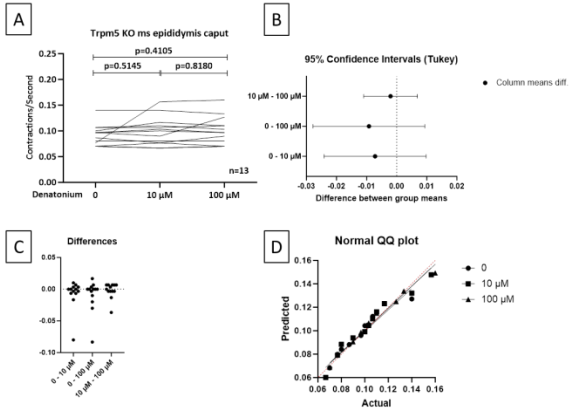

Figure 4-10: *Trpm5 KO* mouse epididymis caput – graphs

Graph B demonstrates that all column means cross the zero value of the x-axis and thus indicating **statistically not significant** results. The data of Tukey's multiple comparison test (Table 4-3) confirms that there is **no statistically significant** outcome for Trpm5 KO mouse epididymis caput.

The differences plot (Figure 4-10C) shows very little volatility as expected around the x-axis.

Being within the 95% confidence interval, the QQ plot confirms the normal distribution of data (Figure 4-10D).

Table 4-3: Tukey's multiple comparison test: Trpm5 KO mouse epididymis caput

Repeated measures one-way ANOVA - Multi comparisons
Trpm5 KO ms epididymis caput - Data

Input

Number of families	1
Number of comparisons per family	3
Alpha	0,05

Output

Tukey's multiple comparisons test	Mean Diff,	95,00% CI of diff,	Below threshold?	Summary	Adjusted P Value	
0 vs. 10 µM	-0,0072	-0,02411 to 0,009758	No	ns	0,5145	A-B
0 vs. 100 µM	-0,0092	-0,02781 to 0,009383	No	ns	0,4105	A-C
10 µM vs. 100 µM	-0,0020	-0,01097 to 0,006890	No	ns	0,8180	B-C

Test details	Mean 1	Mean 2	Mean Diff,	SE of diff,	n1	n2	q	DF
0 vs. 10 µM	0,0921	0,0993	-0,0072	0,0063	13	13	1,5990	12
0 vs. 100 µM	0,0921	0,1013	-0,0092	0,0070	13	13	1,8690	12
10 µM vs. 100 µM	0,0993	0,1013	-0,0020	0,0033	13	13	0,8614	12

4.2.1.4 RM one-way ANOVA for Trpm5 KO mouse epididymis cauda

The one-way ANOVA for Trpm5 KO mouse epididymis cauda showed **no significant** effect of DNT on the frequency of smooth muscle contraction: $F(1{,}531, 13{,}78) = 2{,}844$, $p > 0.05$ (Table 8-7).

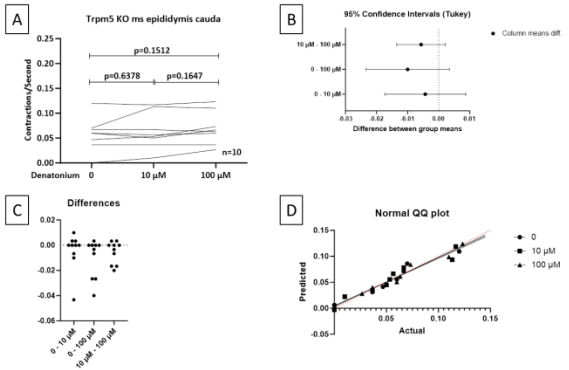

Figure 4-11: Trpm5 KO mouse epididymis cauda – graphs

The differences plot (Figure 4-11C) shows very little volatility around the x-axis and is similar to the differences plot of the Trpm5 KO caput. The Normal QQ plot confirms normal distributed data (Figure 4-11D).

Table 4-4: Tukey's multiple comparison test: Trpm5 KO mouse epididymis cauda

Repeated measures one-way ANOVA - Multi comparisons
Trpm5 KO ms epididymis cauda - Data

Input

Number of families	1
Number of comparisons per family	3
Alpha	0,05

Output

Tukey's multiple comparisons test	Mean Diff,	95,00% CI of diff,	Below threshold?	Summary	Adjusted P Value	
0 vs. 10 µM	-0,0043	-0,01733 to 0,008690	No	ns	0,6378	A-B
0 vs. 100 µM	-0,0100	-0,02344 to 0,003476	No	ns	0,1512	A-C
10 µM vs. 100 µM	-0,0057	-0,01351 to 0,002191	No	ns	0,1647	B-C

Test details	Mean 1	Mean 2	Mean Diff,	SE of diff,	n1	n2	q	DF
0 vs. 10 µM	0,0460	0,0503	-0,0043	0,0047	10	10	1,3110	9
0 vs. 100 µM	0,0460	0,0560	-0,0100	0,0048	10	10	2,9290	9
10 µM vs. 100 µM	0,0503	0,0560	-0,0057	0,0028	10	10	2,8470	9

The Tukey tests for the Trpm5 KO mice -given a 95% confidence interval- demonstrate that there are **no statistically significant** results for the Trpm5 KO mice caput and cauda (Figure 4-10A and B, Figure 4-11A and B).

The results of the RM one-way ANOVA computations confirm the null hypothesis, namely that the Trpm5 cation channel plays a pivotal role in smooth muscle contraction. That means that DNT does **not statistically significant** influence the frequency of smooth muscle contractions in Trpm5 knock-out mice epididymis.

4.2.2 Data testing and outliers

As demonstrated in Table 8-3, all 4 experiments exhibited normal distribution (D'Agostino & Pearson test "omnibus K2 test" (D'Agostino 1973).

All 4 experiments demonstrated the absence of outliners as per the ROUT (Q=1% and 10%, respectively) method as illustrated in Table 4-5, which was generated using Prism GraphPad.

Table 4-5: Outliers set at ROUT 10%

WT caput	**Number of points**	0	10 µM	100 µM
	# Y values analyzed	15	15	15
	Outliers	0	0	0
Trpm5 KO caput	**Number of points**	0	10 µM	100 µM
	# Y values analyzed	13	13	13
	Outliers	0	0	0
WT cauda	**Number of points**	0	10 µM	100 µM
	# Y values analyzed	13	13	13
	Outliers	0	0	0
Trpm5 KO cauda	**Number of points**	0	10 µM	100 µM
	# Y values analyzed	10	10	10
	Outliers	0	0	0

Table 4-6: Data summary

Data summary	WT caput	Trpm5 KO caput	WT cauda	Trpm5 KO cauda
Number of treatments (columns)	3	3	3	3
Number of subjects (rows)	15	13	13	10
Number of missing values	0	0	0	0

As the data summary (Table 4-6) demonstrates, there were no missing values that could have had an adverse impact on the statistical calculations.

4.2.3 Effective matching of experiments

If the matching is effective, the repeated-measures test will yield a smaller P value than an ordinary ANOVA. The repeated-measures test is a very powerful statistical tool as it allows for the separation of between-subject variability from within-subject variability.

Table 4-7: Effective matching of experiments

Was the matching effective?	WT caput	Trpm5 KO caput	WT cauda	Trpm5 KO cauda
F	19,3400	6,6850	14,6000	53,9000
P value	**<0,0001**	**<0,0001**	**<0,0001**	**<0,0001**
P value summary	********	********	********	********
Is there significant matching (P < 0.05)?	**Yes**	**Yes**	**Yes**	**Yes**
R squared	0,8495	0,7495	0,8136	0,9534

The matching for all 4 experiments is effective demonstrating significant match (Table 4-7)

4.2.4 Normal distribution tests

Normal distribution of the underlying data was tested using three different standard methods. All three con-

firmed normal distribution of the underlying data (Table 8-3).

4.2.5 Overview: Statistical significance

As per recommendation by GraphPad, sphericity had not been assumed, as the variances differ between columns. Therefore, the Geisser-Greenhouse's epsilon was computed. In summary, the Geisser-Greenhouse's epsilon leads to a higher P-value, thereby introducing a degree of statistical protection into the calculations. This allows a conservative interpretation of the p-values and thus, supports a robust statement about the results.

Furthermore, the statistical significance is corroborated by a comparison of the F-ratios, which take a 5% confidence interval into account (Table 4-8) with F_{crit} < F-ratio for the wild type mice. F_{crit} is derived from the table shown in Figure 8-3.

The overall results of the 4 RM one-way ANOVA for the four groups (Table 4-8) indicate that there is **no significant** P value for both the Trpm5 KO mice caput and

cauda, respectively. However, the results for the WT mice caput and cauda are **statistically significant**

Table 4-8: RM one-way ANOVA result: Summary

	Trpm5 KO caput	Trpm5 KO cauda	WT caput	WT cauda
Repeated measures ANOVA summary				
Assume sphericity?	No	No	No	No
F-ratio	1,4050	2,8440	9,9850	8,0690
F_{crit}	3,5900	3,7400	3,4400	3,4700
Statistically significant (5% conf. interval)?	No	No	Yes	Yes
P value	**0,2645**	**0,1022**	**0,0016**	**0,0037**
P value summary	**ns**	**ns**	******	******
Statistically significant (P < 0.05)?	**No**	**No**	**Yes**	**Yes**
Geisser-Greenhouse's epsilon	0,6840	0,7656	0,7888	0,8512

As the F-ratio exceeds F_{crit} for WT ms epididymis caput and cauda, the null hypothesis can be rejected and it can be concluded that the differences in group means are **statistically significant** (Table 4-8).

It is evident that the absence of the *Trpm5*-cation channel was the cause of the lack of significant variances in the responses of the smooth muscles to denatonium benzoate, In other words, the contraction patterns of the *Trpm5 KO* mice were **not significantly** affected by

denatonium benzoate (Table 4-9, Figure 4-10, Figure 4-11, Table 8-6, Table 8-7). In contrast, the wild type mice exhibited statistically **significant** frequency changes in their denatonium benzoate-stimulated contraction patterns (Table 4-9, Figure 4-8, Figure 4-9, Table 8-4, Table 8-5).

The Geisser-Greenhouse's epsilon allows evaluating the violation of the assumption of sphericity. The values (Table 4-8) show for Trpm5 KO mice caput a value of 0.6840 which indicates a moderate violation of the sphericity. The value of 0.7656 for Trpm5 KO mice cauda indicates a moderate violation. The values of 0.7888 and 0.8512 for WT mice epididymis caput and cauda indicate almost no violation. That means that the difference for the latter is minimal and should not have an impact on the results of the study.

Details are illustrated in Tukey's multiple comparison test (Table 4-9) and in the previous sections with details for each of the 4 experiments (Table 4-1, Table 4-2, Table 4-3, Table 4-4, Table 8-4, Table 8-5, Table 8-6, Table 8-7).

The differences plots (Figure 4-8C, Figure 4-9C, Figure 4-10C, Figure 4-11C) show higher differences in the contraction patterns for the wild type mice caput and cauda compared to the much smaller differences for the Trpm5 KO mice caput and cauda. This is in line with the expectation confirming the alternative hypothesis that the Trpm5 ion channel is relevant for the contraction pattern of the smooth muscles of the mouse epididymis and thus, higher changes in contraction frequencies of wild type mice epididymis smooth muscles.

Table 4-9: Summary of Tukey's multiple comparison tests

		Mean Diff.	95,00% CI of diff.	Below threshold?	Summary	Adjusted P Value	
WT, caput	0 vs. 10 µM	-0,0151	-0,02493 to -0,005295	Yes	**	0,0033	A-B
	0 vs. 100 µM	-0,0236	-0,03977 to -0,007353	Yes	**	0,0051	A-C
	10 µM vs. 100 µM	-0,0084	-0,02353 to 0,006633	No	ns	0,3361	B-C
Trpm5 KO, caput	0 vs. 10 µM	-0,0072	-0,02411 to 0,009758	No	ns	0,5145	A-B
	0 vs. 100 µM	-0,0092	-0,02781 to 0,009383	No	ns	0,4105	A-C
	10 µM vs. 100 µM	-0,0020	-0,01097 to 0,006890	No	ns	0,8180	B-C
WT, cauda	0 vs. 10 µM	-0,0008	-0,009022 to 0,007469	No	ns	0,9659	A-B
	0 vs. 100 µM	-0,0128	-0,02159 to -0,004068	Yes	**	0,0055	A-C
	10 µM vs. 100 µM	-0,0121	-0,02342 to -0,0006902	Yes	*	0,0375	B-C
Trpm5 KO, cauda	0 vs. 10 µM	-0,0043	-0,01733 to 0,008690	No	ns	0,6378	A-B
	0 vs. 100 µM	-0,0100	-0,02344 to 0,003476	No	ns	0,1512	A-C
	10 µM vs. 100 µM	-0,0057	-0,01351 to 0,002191	No	ns	0,1647	B-C

Note: A = spontaneous contraction; B = 10µM DNT; C = 100µM DNT

5 Discussion

The present study describes a group of epithelial cells in the mouse epididymis appear to constitute a subpopulation of basal cells with tiny cytoplasmatic projections directed towards the lumen (see Figure 4-1) and some reaching the lumen (see Figure 4-3). Moreover, they exhibit chemosensory attributes, expressing components of the taste transduction cascade (Huang et al. 1999; Shum et al. 2008). A screening of mouse epididymis sections revealed that only a small number of basal cells reach the lumen. Additionally, Shum et al. (2008) characterized these basal cells as dynamic properties subject to a local regulation in different regions of the epididymis. In other words, this slender cytoplasmatic projection is developed when necessary. It has been previously described that basal cells initially emerge in the basal region of the duct epithelium during postnatal development. However, over time they can be found in the upper sections as well (Seiler et al. 1998). In the rat epididymis, the first observation of a basal cell with a luminal projection was made after postnatal week 8 (Shum et al. 2013). This capacity of basal cells to

reach the lumen is described as a property that varies across different regions of the epididymis (Shum et al. 2013). Tuft cells, which are also known as brush cells, have been described as differentiated basal cell population in other organs, such as the tracheal epithelium (Saunders et al. 2013). Additionally, they have been observed to co-express *Trpm5*, *ChAT* and *Gα-gustducin, also known as GNAT3* (Saunders et al. 2013). Moreover, Dorscht (2020) identified the chemosensory characterization of the non-neuronal-cholinergic cells of the epididymal epithelium by detecting components of the taste transduction cascade. These brush cells have been repeatedly documented in many other organs, including the respiratory and gastrointestinal tracts, as well as the urethra (Krasteva et al. 2011; Deckmann et al. 2014; Schütz et al. 2015).

The present study confirms the existence of basal cells with slender cytoplasmic projections extending to the lumen (see Figure 4-1) and in rare cases until the lumen (see Figure 4-3).

The presence of numerous components of the taste cascade, including the taste receptor *Tas2r108, Plcb,*

and the *Trpm5* cation channel, has been observed in the epididymis (Dorscht 2020). The latter facilitates the influx of Na^+, which depolarizes a calcium channel, allowing the influx of Ca^{2+} and ultimately leading to smooth muscle contraction.

Denatonium benzoate, a bitter compound, has been demonstrated to bind to the taste receptor (Huang et al. 1999), predominantly on the *Tas2r108 (Chandrashekar et al. 2000; Foster et al. 2014)*. It affects the spontaneous contractility of the epididymal duct's smooth muscle cells (see Table 4-9, Figure 4-8, Figure 4-9). The smooth muscle cells of the epididymis are responsible for the transport of spermatozoa, which could be influenced by different drugs (Mewe et al. 2006a; Mietens et al. 2014). During this research, the described denatonium benzoate effect was observed at an absolute concentration of 10 µM and resulting in a significant frequency change of the spontaneous contraction of the epididymal duct (see Table 4-9, Figure 4-8, Figure 4-9) in wild type mice. It is likely that this effect is dependent on the epididymal brush cells, which appear to activate the smooth muscle layer that surrounds the epithelium.

Additionally, brush cells in other organs, such as the trachea and urethra have been shown to influence the contraction of smooth muscle cells (Krasteva et al. 2011; Deckmann et al. 2014) and the epithelial defense program (Perniss et al. 2023).
A comparable frequency change was not observed in the *Trpm5 KO* mouse epididymal duct (see Table 4-9, Figure 4-10, Figure 4-11).

These findings align with those of Damak et al. (2006), who observed a diminished response to bitter compounds in the tongues of *Trpm5 KO* mice (Damak et al. 2006; Banik et al. 2018).

The co-expression of Trpm5 and Tas2r has been previously demonstrated (Zhang et al. 2003). The *Trpm5* cation channel has been confirmed in the epididymis (Dorscht 2020).

It has been demonstrated that *Tas2r* bitter receptors are co-expressed with *Gα*- gustducin and that they can activate this G protein in vitro (Chandrashekar et al. 2000). Additionally, *Tas2r108* has been demonstrated to

function as an agonist of denatonium benzoate eliciting a robust Ca^{2+} response (Foster et al. 2014).

5.1 Impact by material and methods

5.1.1 Critical evaluation of this research project

5.1.1.1 Immunohistology: Strengths and limitations

The immunohistochemistry technique is a valuable tool for identifying cell or tissue antigens, which can be specific to a range of amino acids, proteins, and cells. However, it is not without limitations.

The analysis of the tissue is conducted in two steps:

1. Preparation of the slides including the stages involved in the reaction, and
2. Interpretation and quantification of the obtained expression.

“The acquisition, handling, fixation, specimen delivery to the laboratory and antigen retrieval are all critical factors.” (Matos et al. 2010).

In the present study, 6 µm thick tissue slices and the aforementioned protocol were used by our research group during the past couple of years. Consequently, the primary constraints are attributable to deficiencies in the handling process. Keratin5 proved highly effective in identifying basal cells. Also, as previously described (Shum et al. 2008), there are several cells with slender processes towards the lumen, i.e. a subpopulation of basal cells. In searching for cells where the cytoplasmic projection reaches the lumen, it is possible that the number of aforementioned cells reaching the lumen may be greater than observed, as the sample may have been cut prior to reaching that area. The shape of the basal cells is similar to a pyramid. When cutting 6µm sections visualizing the wide basis is much more likely compared to the slender apical part of these cells in the same sample.

The co-expression was observed between keratin5 and COX1 (not shown), keratin5 and GNAT3 (see Figure 4-2) as well as keratin5 and Dclk1 (see Figure 4-3).

The aforementioned marker proteins for tuft cells and their co-expression were previously shown in other

organs: It has been suggested that cells expressing Trpm5, which are believed to be tuft cells, were previously shown to express the cyclooxygenase 1 and 2 (COX1 and COX2) enzymes (Bezençon et al. 2008). Additionally, recent findings indicate that the expression of the Dclk1 protein serves as a specific marker for tuft cells (Gerbe et al. 2011).

This research can be compared with a study about the intestinal epithelial cells. It has been suggested that Dclk1 plays a critical functional role in the epithelial restorative response (May et al. 2014). Furthermore, it has been established that Dclk1-expressing tuft cells influence the regulation of the entire intestinal epithelial cell population following injury through a paracrine mechanism. These findings imply that intestinal tuft cells are important in regulating the ATM (ataxia-telangiectasia mutated) mediated DNA damage response, contributing to epithelial cell survival and self-renewal via a Dclk1-dependent process. These mechanisms are considered essential for restitution and proper function following severe radiation-induced injury (Chandrakesan et al. 2016).

Tuft cells, which express Dclk, form a distinct intestinal epithelial lineage separate from enterocytes, Paneth cells, goblet cells, and enteroendocrine cells. These cells are characterized by the expression of taste-related receptors, specific transcription factors, and their close interactions with the enteric nervous system, hinting at their role in chemosensation. Recent studies have also highlighted their interaction with immune system cells, suggesting they play a critical part in regulating responses to intestinal parasites. Furthermore, the removal of tuft cells significantly hinders epithelial proliferation and tissue regeneration after injury, indicating their involvement in modulating epithelial stem and progenitor functions. Additionally, tuft cells expand in conditions of chronic inflammation and in preneoplastic tissues, suggesting they might play an early role in inflammation-driven tumorigenesis. The evidence points to tuft cells as essential regulators within the intricate network of the intestinal microenvironment (Middelhoff et al. 2017).

5.1.1.2 Time-lapse imaging: Strengths and limitations

Time-lapse imaging offers a valuable approach for systematically evaluating and studying contraction patterns of smooth muscles in diverse organs over extended periods.

The frequency of spontaneous smooth muscle contractions in the epididymal duct could be visualized by creating a reslice using ImageJ (see Figure 3-2A and B, Table 3-1). The reslice may be employed for the purpose of computing the contraction frequency. However, merely observing the video without creating a reslice does not yield reliable data regarding the contraction pattern and frequency.

As demonstrated by the findings of our research group, time-lapse imaging is a reliable tool for both shorter (minimum of 5 minutes) and longer observation periods (Mietens et al. 2014, Kügler et al. 2018).

Collagen serves to fix the prepared tissue sample without restricting its movement. The application of heating electrodes ensures that the temperature of the sur-

rounding environment is within physiological range. In comparison to organ bath studies, there is no necessity to:

1. Clamp the tissue between two clamps, and
2. Establish a pretension following the clamping of the tissue.

Both procedures have the potential to alter the tissue and consequently, its function. Nevertheless, organ bath studies offer certain advantages over time-lapse imaging. These include the possibility of parallel analysis of several tissue samples, the directly measurable amplitude, and the simple inflow and outflow of administered substances. It has repeatedly been mentioned that the tissue sample from the caput is too fragile to be clamped in an organ bath different to the cauda. Accordingly, time-lapse imaging was selected as the optimal methodology.

Two different *Trpm5 KO* mice (designated as S and Y) did not show any contraction over the observation period for the cauda (segment 8), while the caput (segment 2) of the epididymis demonstrated a normal, i.e. ex-

pected, contractility pattern for both animals. However, all four tissues exhibited normal physiological responses at the conclusion of each experiment following the administration of noradrenaline. As the tissue was meticulously dissected, it can be definitely stated that the very distal part, i.e., the most distal part of the cauda epididymis (segment 10), which does not exhibit spontaneous contractions, was not inadvertently utilized.

To eliminate potential bias, all conducted experiments, including those involving the aforementioned two different mice (cauda of animal S and Y), were included in the analysis (see Table 8-1). It can be reasonably assumed that the cauda of mice S and Y should also possess a *Tas2r108* receptor and/or the *Trpm5* cation channel, given that the caput of both mice (S and Y), exhibited normal contraction patterns after application of DNT. It appears that the observed contraction frequencies in both mice were prolonged, exceeding the time of the experimental setup. However, this is in contrast with the expectation that the contraction frequency of the cauda should be lower compared to the caput (see Figure 1-4) and cannot be explained.

5.1.2 Different experimental setups

As there are no contraction studies on mouse epididymis with bitter substances and taste transduction cascade, it is challenging to directly compare the results of this study with existing literature.

Nevertheless, to reach a conclusion, it is possible to compare the results to experiments that examine the same species with analogous genes (wild type, *Trpm5 KO*) but different organs, comparable taste transduction cascades, and which use bitter compounds such as denatonium benzoate. In their respective studies Zhang et al.(2003) and Banik et al.(2018) utilized the tongues of wild type and *Trpm5 KO* mice, employing denatonium benzoate as their experimental agent.

5.1.3 Different biochemical and physiological aspects

It was demonstrated that only with a double knockout of *Trpm4* and *Trpm5,* the sensitivity to denatonium benzoate was eliminated completely (Banik et al. 2018). This may confirm the observation in this thesis that some

Trpm5 KO mice exhibit a minimal –but not statistically significant- response to denatonium benzoate (Damak et al. 2006) following its administration (see Figure 4-10, Figure 4-11, Table 8-1).

Tas2r108, a known bitter receptor has been observed to elicit a response in mice to denatonium benzoate (Avau et al. 2015; Chandrashekar et al. 2000; Gulbransen et al. 2008). Nevertheless, other researchers have questioned the potency of denatonium on the *Tas2r108* receptor, while maintaining that it may still exert an effect in general (Lossow et al. 2016).

This study demonstrates that denatonium benzoate has an effect when applied (see Figure 4-6, Figure 4-7, Figure 4-8, Figure 4-9, Table 4-1, Table 4-2 , Table 4-8, Table 4-9,Table 8-3) to tissue of wild type mouse epididymis.

5.1.4 Different concentrations

As demonstrated by Zhang et al. (2003), the knockout of the *Trpm5* ion channel results in a statistically significant reduction in the response to bitter stimuli when dena-

tonium benzoate is used. Also Banik et al. (2018) demonstrated that denatonium benzoate can serve as an activator of the *Trpm5* cation channel. It was demonstrated that mice lacking the *Trpm5* ion channel retained some sensitivity to bitter taste qualities when exposed to concentrations above 1 mM (Banik et al. 2018).

The concentrations utilized in this study are 10 µM and 100 µM, respectively, on mouse epididymis tissue (see Table 8-1 and Table 8-2) and thus are well below the aforementioned concentrations.

However, direct comparison of the concentrations is not possible, as different organs and tissues may require different triggers. Furthermore, other experiments employ licking tests or Ca-imaging experiments which introduce additional variables.

The aforementioned experiments did not yield sufficient evidence to confirm whether higher concentrations exert an inhibitory effect (Prawitt et al. 2003).

In the present study, even a concentration of 1 mM (data not shown) demonstrated increased frequencies,

typically reaching such high amounts which could not be quantified.

5.1.5 Comparison of results with available literature

A review of the literature indicates that no similar statistical analysis had been conducted on the epididymis of a mouse yet. Thus, the presence of the *Trpm5* cation channel (see Figure 2-1) in the epididymis of a mouse has been previously demonstrated (Dorscht 2020). To the best of my knowledge, no comparable statistical analysis and results have been published on the influence of the Trpm5 cation channel on smooth muscle contraction in the epididymis.

Following the removal of the epithelium from the duct of the mouse epididymis, the number of spontaneous contractions is significantly reduced (Mewe et al. 2006a). This suggests the existence of epithelial factors influencing smooth muscle contraction.

Additionally, experimental evidence indicates that the removal of all luminal content from the epididymis af-

fects smooth muscle contraction, specifically the cGMP pathway (Mewe et al. 2006a).

The signaling transduction of *Trpm5* cation channels remains unclear (Balemans et al. 2017). However, chemosensory cells in the urethra (Deckmann and Kummer 2016) and other organs, as previously mentioned, have been identified. Additionally, taste receptors such as *Tas2r108* have also been studied (Wu et al. 2005; Avau et al. 2015).

Taste receptors such as *Tas2r108* can be triggered by denatonium benzoate (Chandrashekar et al. 2000; Xu et al. 2013; Bachmanov et al. 2014). The respective *Tas2r108*-expressing cells may also contain a *Trpm5* cation channel (Hofmann et al. 2003), which is necessary for the transduction of bitter sensing (Clapp et al. 2001; Pérez et al. 2002; Zhang et al. 2003; Banik et al. 2018; Kanehisa Laboratory in Kyoto University 2022).

Moreover, to the best of my knowledge, no study has yet examined the effect of denatonium benzoate on the contraction of the epididymis in wild type and *Trpm5 KO* mice in order to demonstrate the statistical significance.

However, Silva Júnior da, E. D. et al. (2014) demonstrated in vitro and in vivo contraction effects utilizing clonidine in the distal cauda epididymis. The administration of clonidine was observed to increase the frequency of contraction (Silva Júnior da, E. D. et al. 2014).

The signal transduction of the bitter receptor in mammals has been the subject of several studies (Huang et al. 1999). Nevertheless, such research has yet to be conducted in regard to the epididymis.

The present study demonstrated that the signal transduction appears to be analogous to the bitter taste receptor *Tas2r108* in the tongue. Therefore, it can be postulated that the contraction of smooth muscle cells in response to bacterial, viral, or other stimuli (such as denatonium benzoate) may serve to protect the body against ascending infection. The presence of basal cells, which reach the lumen (see Figure 4-1), as well as positive results on various markers (keratin5) accompanied by positive immunohistological studies using Dclk1 (see Figure 4-3) and GNAT3 (see Figure 4-2) antibodies lead to the conclusion that the epithelium of the mouse epididymis contains brush cells or brush cell-like cells.

5.2 Statistical results

The results of the RM one-way ANOVAs corroborate the hypothesis that the Trpm5 cation channel plays a pivotal role in smooth muscle contraction, thereby safeguarding the organism against foreign bodies. In light of the aforementioned results, it can be postulated that *Trpm5* cation channels represent a category of epithelial factors that exert influence over smooth muscle contractions within the epididymis of a mouse. This conclusion can be derived from the **statistically significant** results for the wild type mouse (see Table 4-8, Table 4-9, Figure 4-8, Figure 4-9) and as expected the (**not statistically significant**) results of the *Trpm5 KO* mouse (see Figure 4-10, Figure 4-11).

Potential explanations are:

- **Caput (segment 2)**: The caput of the wild type mouse exhibits a **statistically significant** disparity between spontaneous contraction and contraction subsequent to the administration of denatonium benzoate, even at a low dose of 10 µM. This could be attributed to the reduced muscular mass and/or

augmented receptor density observed in this region (see Figure 4-8).

- **Cauda (segment 8)**: It could be possible that the thicker layer and higher muscle mass necessitates a greater dosage of denatonium benzoate to achieve a **statistically significant** change in the contraction frequency of WT mice epididymis. **Statistically significant** differences were observed between spontaneous contraction and higher concentrations (10 µM vs. 100 µM) of denatonium benzoate, respectively (see Figure 4-9).
- Additionally, it is noteworthy that the caput exhibits 3 times the number of basal cells compared to the corpus and cauda (Shi et al. 2021).

It is evident that the absence of the *Trpm5*-cation channel was the cause of the lack of significant variation in responses by the smooth muscle cells upon the application of denatonium benzoate (Table 4-8: RM one-way ANOVA result: Summary,Table 4-9: Summary of Tukey's multiple comparison tests).

The presence of the *Trpm5* cation channel may serve as a protective mechanism for an essential organ such

as the epididymis, which is crucial for sperm maturation (Hollenhorst and Krasteva-Christ 2023; Krasteva et al. 2012; Perniss et al. 2020).

This chemosensory ability of cells was recently described as a bacterial sensing mechanism that enables the detection of pathogens and harmful substances in the environment (Perniss et al. 2020). Irritants such as acyl–homoserine lactone bacterial quorum-sensing molecules for Gram-negative bacteria appear to utilize the same pathway as bitter compounds via the taste transduction cascade (Tizzano et al. 2010; Finger et al. 2003; Saunders et al. 2014).

As investigated by our working group previously, the epididymal duct responds to bacterial infection in a segmental manner by tightening the segment directly apical to the ascending bacterial-infected segment (Stammler et al. 2015). This may be the result of smooth muscle contraction initiated by *Trpm5* cation channels or *ChAT*-expressing cells detecting harmful luminal fluid.

The aforementioned brush cell-like basal cells, which were identified in the epithelium exhibit analogous de-

fensive mechanism characteristics to those observed in other chemosensory cells located in the tongue, respiratory and gastrointestinal tracts, as well as the urethra (Shum et al. 2008; Schütz et al. 2015; Deckmann and Kummer 2016; Kummer and Deckmann 2017).

Nevertheless, the precise signal transduction mechanism by which the basal cell interacts with the *Trpm5* cation channel to regulate smooth muscle function remains unclear.

The results of this study may lead to the formulation of two hypotheses regarding the smooth muscle contraction of the isolated parts of the epididymal duct in the experimantal setup (without contact to the central nervous system):

- The calcium efflux may trigger the motoric unit of the smooth muscle cells.
- In light of the aforementioned research findings, it can be postulated that the signal transduction in the mouse epididymis to the smooth muscle cells may occur via direct transmission

by acetylcholine or the eNOS pathway or via an yet unknown pathway.

In approximately 3% of men, the defense mechanism of the epididymis is ineffective resulting in ascending UTI. It is currently unclear whether there is a relationship between the *Tas2r108* receptor and the *Trpm5* cation channel in the brush cell-like basal cells. If there is a failure in these receptors, it may result in a lack of contraction and subsequent inability to expel foreign bodies. The results presented above suggest that the contractions of the epididymal duct's smooth muscles are dependent on the functionality of the *Trpm5* cation channel (Table 4-8: RM one-way ANOVA result: Summary,Table 4-9: Summary of Tukey's multiple comparison tests).

It can be posited that the *Trpm5* receptor is present exclusively in the epithelium of the epididymis and not in the smooth muscle layer itself (Dorscht 2020).

The results of the present work indicate that the Trpm5 receptor is a crucial factor in smooth muscle contraction

and plays a pivotal role in the defense mechanism of the mouse epididymis.

It may be worthwhile to investigate whether male humans who have experienced a urinary tract infection (UTI) possess an intact ability to perceive bitter tastes. This is due to a potential correlation between the malfunction of the *Trpm5* cation channel and/or the human Tas receptor, *T2R38,* and the vulnerability by ascending infections.

Consequently, further research in these areas may facilitate a more comprehensive understanding of the underlying causes of UTI.

6 Summary

The primary objective of this research is to compare the contraction characteristics of the smooth muscles of the epididymis between wild type and *Trpm5* KO mice. This is done in order to verify the hypothesis that the gustatory signal cascade, specifically the epithelium-specific ion channels, namely the *Trpm5* cation channels, is essential for contraction and therefore plays a crucial role in the defense mechanism of the epididymis.

The null hypothesis is that there will be **no statistically significant** impact of denatonium benzoate on the contraction pattern of *Trpm5 KO* mice, while it is expected that there will be a **statistically significant** increase in the contraction pattern of the smooth muscles of the epididymis of wild type mice.

In approximately 3% of men, the defense mechanism fails, resulting in the development of ascending UTI. It is currently unclear whether there is a relationship between the *Tas2r108* (or *Tas2r38* in humans) receptor and the *Trpm5* cation channel of the brush cell-like basal cells. If such a relationship exists, it would explain

why contraction is not triggered to squeeze out foreign bodies with a defect Trpm5 cation channel.

6.1 Methods

By immunohistological double staining, the co-expression of elements of the transduction signaling cascade could be demonstrated for basal cells with Dclk1 and GNAT3, respectively (see Figure 4-2, Figure 4-3).

The results of the time-lapse imaging experiments demonstrated a **statistically significant** effect on the contraction pattern of wild type mice, while **no significant** effect was observed in *Trpm5 KO* mice.

6.2 Statistical results

The statistical results based on the time-lapse imaging suggest that the contractions of the epididymal duct's smooth muscles are dependent on a functioning *Trpm5* cation channel (see Table 4-8: RM one-way ANOVA result: Summary,Table 4-9: Summary of Tukey's multiple comparison tests).

6.3 Conclusion

The increased contractility of the epididymal duct of WT epididymis caput and cauda triggered by higher concentration of the bitter compound denatonium benzoate is dependent on the presence of a functioning *Trpm5* cation channel. This finding is significant in terms of the defense system of the epididymal duct against foreign bodies, and thus in the context of ascending UTI.

7 Zusammenfassung

Das Hauptziel dieser Untersuchung ist der Vergleich der Kontraktionseigenschaften der glatten Muskulatur des Nebenhodens zwischen Wildtyp- und *Trpm5*-KO-Mäusen, um unsere Erwartung zu überprüfen, dass die gustatorische Signalkaskade, d.h. die epithelspezifischen Ionenkanäle, nämlich die Trpm5-Kationenkanäle, der Schlüssel zur Kontraktion und damit zum Abwehrmechanismus des Nebenhodens sind.

Als Hypothese wird erwartet, dass das Kontraktionsmuster der glatten Muskeln der Nebenhoden keine statistisch signifikante Auswirkung von Denatoniumbenzoat auf das Kontraktionsmuster der *Trpm5*-KO-Mäuse gibt von während es bei Wildtyp-Mäusen signifikant ansteigt.

Bei etwa 3 % der Männer versagt der Abwehrmechanismus, so dass sie an einer ständig wiederkehrenden Harnwegsinfektion leiden. Es ist nicht bekannt, ob ein Zusammenhang mit dem Tas2r108-Rezeptor (bzw. entsprechend *Tas2r38* im Menschen) oder dem Trpm5-Kationenkanal der bürstenzellartigen

Basalzellen besteht, so dass die Kontraktion nicht ausgelöst wird, um Fremdkörper herauszudrücken bei defektem Trpm5-Kationenkanal.

7.1 Methoden

Durch immunhistologische Doppelfärbung konnte die Koexpression von Elementen der Transduktionssignalkaskade für Basalzellen mit Dclk1 bzw. GNAT3 nachgewiesen werden (siehe Figure 4-2, Figure 4-3).

Mit Time-Lapse-Imaging-Experimenten konnte nachgewiesen werden, dass es einen **signifikanten** Effekt auf das Kontraktionsmuster von Wildtyp-Mäusen gibt, aber der Effekt statistisch **nicht signifikant** für *Trpm5 KO*-Mäusen ist.

7.2 Statistische Ergebnisse

Die statistischen Ergebnisse auf der Grundlage der Zeitrafferaufnahmen deuten darauf hin, dass die Kontraktionen der glatten Muskulatur des Nebenhodenkanals von einem funktionierenden Trpm5-Kationenkanal abhängig sind (siehe Table 4-8: RM one-way ANOVA

result: Summary,Table 4-9: Summary of Tukey's multiple comparison tests).

7.3 Schlussfolgerung

Die Erhöhung der Kontraktilität des Nebenhodenganges (Caput und Cauda) durch den Bitterstoff Denatoniumbenzoat ist abhängig vom Vorhandensein des funktionierenden Trpm5-Kationenkanals. Dies dürfte für das Abwehrsystem des Nebenhodenganges gegen Fremdkörper und damit aufsteigende Harnwegsinfekte von Bedeutung sein.

8 Appendix

8.1 List of Abbreviations

8-Br-cGMP	***8-Bromoguanosine 3',5'-cyclic monophosphate***
ANOVA	***Analysis of Variance***
ATP	***Adenosine triphosphate***
ATPase	***Adenosine triphosphatase***
C57BL/6N	***C57 black substain 6 mouse***
Ca^{2+}	***Calcium ion***
CBF	***Ciliary beat frequency***
CCC	***cholinergic chemosensory cells***
cGMP	***Guanosine 3',5'-cyclic monophosphate***
ChAT	**Choline acetyltransferase**
COX-1	**Cyclooxygenase 1**
Cs^{+}	***Cesium ion***
DAG	**Diacylgycerol**
DAPI	**4',6-Diamidine-2'-phenylindole dihydrochloride**

DCLK1	**Doublecortin like kinase 1**
DMEM	***Dulbecco's Modified Eagle's Medium***
DNT	***Denatonium benzoate, Denatonium benzoate, Denatonium benzoate***
eNOS	***endothelial nitrogen monoxide synthase***
ER	**Endoplasmic reticulum**
FDR	***False Discovery Rate***
Gbeta1	***Guanine nucleotide-binding protein G subunit beta-1***
Ggamma13	***Guanine nucleotide-binding protein G subunit gamma-13***
GNAT3	**Guanine nucleo-tide-binding protein G(t) subunit alpha-3**
Gq	**Phospholipase C-coupled G-protein**
HEPES	***4-(2-hydroxyethyl)-1-piperazineethanesulfonic acid***
IP3	**Inositoltripsphosphat**
K^+	***Kalium ion***

Keratin5	**Cytokeratin5**
KO	***knock-out***
MEM	***Minimal essential medium***
ms	***mouse***
Na	**Natrium**
Na^+	***Natrium ion***
NaOH	***Natriumhydroxide***
NE	***Noraderenaline***
NO	***Nitrogen monoxide***
nt	***Nucleotid***
PBS	**Phosphate Buffered Saline: 0,136M NaCl and 0,05M Na2HPO4 with HCl set at pH 7,4**
PFA	***Paraformaldehyde***
PLC	**Phospholipase C**
ppm	***parts per million***
RM	***Repeated Measures***
ROUT	***Robust regression and outlier removal method***
RT-PCR	***Reverse transcriptase-PCR***

sec	***seconds***
T1R	***Taste receptor type 1***
T2R	***Taste receptor type 2***
T2R108	***Taste receptor type 2 member 108***
TRPM5	***Transient receptor potential melastin isoform 5 ion channel***
UTI	**Urinary tract infection**
WT	***wild type***

8.2 List of Tables

8.3 List of Illustrations

8.4 Protocol immunostaining - example

Immunofluoreszenz - Paraffin

Datum: 8./9.10.2019 Protokoll-Nr.: 50/19
Material: NH, ms WT Name: Dirk
231/17-3
Nr. 44, 45, 56, 51, 63, 77

1. Entparaffinieren:

- Xylol	3 x 5 Min.	
- 100% EtOH	5 Min.	
- 96% EtOH	5 Min.	
- 70% EtOH	5 Min.	
- Aqua dest	5 Min.	
- ggfs. Citratpuffer in Microwelle (abhängig vom Antikörper)	kochen (750W), danach 15 Min. (450W)	GNAT3
- PBS	5 Min.	

2. Blockung: 2% Normal Goat (oder Horse) Serum (40µl + 1960µl PBS) — 1 Std., RT

3. Primärantikörper (in Verdünnungspuffer ("VP"): PBS + 0,2% BSA + 0,1% NaN_3): — über Nacht, 4°C

Objekt-träger	#	Antikörper	Source	Vorverdünnung/pur (1:1)		Verdünnung		AK	VP
44	1	GNAT3	gt	1	10	1	800	3	237
45	2	DCLK1	rb	1	10	1	1.000	3	297
56	3	VAChT	gt	1	2	1	8.000	1	3.999
51	4	Keratin5	rb	1	1	1	200	2	398
	4	GNAT3	gt	1	10	1	800	5	395
									393
63	5	VAChT	gt	1	2	1	8.000	0,125	500
	5	Keratin5	rb	1	1	1	200	2,5	498
									497
77	6	VAChT	gt	1	2	1	8.000	0,125	500
	6	DCLK1	rb	1	10	1	1.000	5	495
									495

Kontrollen: jeweils Verdünnungspuffer

4. Waschen: PBS — 2 x 10 Min.

ab hier ist alles Lichtempfindlich !!!!!

5. Sekundärantikörper (S-AK) auf alle Schnitte:

#	Antikörper	Source	Vorverdünnung/pur (1:1)		Verdünnung		AK	PBS
A	Alexa (grün)	dk-a-gt	1	2	1	400	8,5	1.692
A	Cy311 (rot)	dk-a-rb	1	2	1	400	8,5	1.692
A	DAPI (blau)		1	1	1	1.250	1,3	1.624
	-->Zentrifugieren!!!							**1.682**

	Anzahl Schnitte	µl S-AK/Schnitt	Menge Sek-AK
Benötigte Menge Sek-AK	24	70	**1680**

1 Std., RT (dunkel)

6. Waschen:	PBS	2 x10 Min
	4% PFA	10 Min
	PBS	2 x10 Min
7. Eindeckeln:	gep. Glycerol	Aufbewahrung: 4°C (dunkel)

Figure 8-1: Protocol immunostaining

Source: AG Middendorff

8.5 Protocol “Time-lapse imaging”

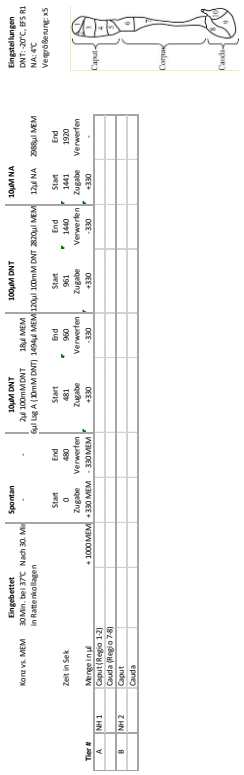

Figure 8-2: Protocol template "time-lapse imaging"

8.6 Raw data "Time-lapse imaging"

Table 8-1: Contraction study: Trpm5 knock-out mice, epididymis

				no treatment			10µM denatonium			100µM denatonium			10µM noradrenaline	
Date	Animal #	Tissue (Caput 1-2, Cauda 7-8)	Filename	Sequency	Contractions per 5 minutes	Contactions /sec	Sequency	Contractions per 5 minutes	Contactions /sec	Sequency	Contractions per 5 minutes	Contactions /sec	Sequency	Alive
14.09.18	A	Caput	Re slice Tier A of 180914 Film 1	60-360	21	0,0700	550-850	20	0,0667	1080-1380	21	0,0700	2110-2410	Yes
14.09.18	A	Cauda	Re slice Tier A 180914 Bild 2 Cau 1a auszae hi	60-360	21	0,0700	560-860	34	0,1133	1070-1370	33	0,1100	2110-2410	Yes
14.09.18	B	Caput	Re slice Tier B Film5 Cap2	60-360	21	0,0700	560-860	20	0,0667	1070-1370	21	0,0700	2150-2450	Yes
14.09.18	C	Caput	Re slice Tier C 190914 Film 7 Cap 3	60-360	26	0,0867	560-860	23	0,0767	1060-1360	21	0,0700	2090-2390	Yes
14.09.18	C	Cauda	Re slice Tier C 190914 Film 8 Cau 3	60-360	36	0,1200	550-850	35	0,1167	1040-1340	37	0,1233	2070-2370	Yes
20.02.19	P	Caput	Re slice of 190220 Caput 2a	60-360	32	0,1067	560-860	32	0,1067	1100-1400	33	0,1100	1505-1805	Yes
20.02.19	P	Cauda	Re slice of 190220 Cauda 1a	60-360	20	0,0667	600-900	20	0,0667	1100-1400	19	0,0633	1505-1805	Yes
07.03.19	R	Caput	Re slice of 190307 Caput 2a	60-360	32	0,1067	550-850	33	0,1100	1030-1330	31	0,1033	1505-1805	Yes
08.03.19	S	Caput	Re slice of 190308 Caput 1a	60-360	29	0,0967	550-850	30	0,1000	1030-1330	29	0,0967	1505-1805	Yes
08.03.19	S	Cauda	Re slice of 190308 Cauda 2a	60-360	0	0,0000	550-850	0	0,0000	1030-1330	0	0,0000	1600-1900	Yes
11.03.19	T	Caput	Re slice of 190311 Caput 2b	60-360	24	0,0800	550-850	24	0,0800	1030-1330	24	0,0800	1505-1805	Yes
11.03.19	T	Cauda	Re slice of 190311 Cauda 2b	60-360	14	0,0467	550-850	16	0,0533	1030-1330	22	0,0733	1505-1805	Yes
13.03.19	U	Caput	Re slice of 190313 Caput 1a	60-360	29	0,0967	550-850	31	0,1033	1250-1550	29	0,0967	1730-2030	Yes
13.03.19	U	Cauda	Re slice of 190313 Cauda 2b	60-360	0	0,0000	610-910	3	0,0100	1030-1330	8	0,0267	1505-1805	Yes
14.03.19	V	Caput	Re slice of 190314 Caput 2b	60-360	42	0,1400	550-850	42	0,1400	1030-1330	40	0,1333	1505-1805	Yes
11.01.19	X	Caput	Re slice of NH2 Cap	60-360	29	0,0967	550-850	27	0,0900	1030-1330	38	0,1267	1505-1805	Yes
11.01.19	X	Cauda	Re slice of NH2Cau	60-360	11	0,0366	550-850	11	0,0366	1030-1330	11	0,0366	1505-1805	Yes
11.01.19	Y	Caput	Re slice of NH1 Cap	60-360	23	0,0767	550-850	47	0,1567	1030-1330	48	0,1600	1505-1805	Yes
11.01.19	Y	Cauda	Re slice of NH1Cau	60-360	0	0,0000	550-850	0	0,0000	1030-1330	0	0,0000	1505-1805	Yes
19.01.19	Z	Caput	Re slice of NH1 Cap	60-360	30	0,1000	550-850	35	0,1167	1030-1330	33	0,1100	1505-1805	Yes
19.01.19	Z	Cauda	Re slice of NH1Cau	60-360	18	0,0600	550-850	15	0,0500	1030-1330	20	0,0666	1505-1805	Yes
27.01.19	AB	Caput	Re slice of NH1 Cap	60-360	21	0,0700	550-850	23	0,0767	1030-1330	27	0,0900	1505-1805	Yes
27.01.19	AB	Cauda	Re slice of NH1Cau	60-360	18	0,0600	550-850	17	0,0566	1030-1330	18	0,0600	1505-1805	Yes

Intentionally left blank

Table 8-2: Contraction study: Wild type mice, epididymis

				no treatment			10µM denatonium			100µM denatonium			10µM noradrenaline	
Date	Animal #	Tissue (Caput 1-2, Cauda 7-8)	Filename	Sequency	Contractions per 5 minutes	Contactions /sec	Sequency	Contractions per 5 minutes	Contactions /sec	Sequency	Contractions per 5 minutes	Contactions /sec	Sequency	Alive
24.09.18	D	Caput	180924 Reslice of 3.tif	60-360	29	0,0967	550-850	34	0,1133	990-1290	32	0,1067	2315-2615	Yes
24.09.18	D	Cauda	nicht auswertbar	60-360	0	0,0000	550-850	0	0,0000	990-1290	0	0,0000	2315-2615	Yes
24.09.18	E	Caput	nicht auswertbar	60-360	41	0,1367	520-820	0	0,0000	990-1290	0	0,0000	2315-2615	Yes
25.09.18	F	Caput	1 Cap1 Reslice Film 3 Bil 1.tif	60-360	28	0,0933	550-850	42	0,1400	920-1220	44	0,1467	1840-2140	Yes
25.09.18	F	Cauda	Reslice Film 4.tif	60-360	16	0,0533	540-840	18	0,0600	1000-1300	19	0,0633	2030-2330	Yes
25.09.18	G	Caput	Reslice Film 5.tif	60-360	27	0,0900	570-870	37	0,1233	1000-1300	31	0,1033	2030-2330	Yes
01.10.18	H	Cauda	Reslice 4 Cauda 1b final.tif	60-360	15	0,0500	550-850	20	0,0667	910-1210	24	0,0800	2315-2615	Yes
02.10.18	I	Cauda	2 Cauda 1a.tif	60-360	8	0,0267	630-930	9	0,0300	1100-1400	14	0,0467	2020-2320	Yes
02.10.18	I	Caput	nicht auswertbar	60-360	0	0,0000	520-820	0	0,0000	990-1290	0	0,0000	2315-2615	Yes
08.10.18	J	Caput	Caput 1a.tif	60-360	28	0,0933	540-840	38	0,1267	910-1210	29	0,0967	2030-2330	Yes
08.10.18	J	Cauda	Cauda 1a.tif	60-360	7	0,0233	600-900	7	0,0233	980-1280	5	0,0167	1990-2290	Yes
11.10.18	K	Cauda	Cauda 1a.tif	60-360	8	0,0267	560-860	7	0,0233	1030-1330	9	0,0300	1510-1810	Yes
11.10.18	K	Cauda	Cauda 1a.tif	60-360	12	0,0400	570-870	15	0,0500	1040-1340	15	0,0500	1520-1820	Yes
15.10.18	L	Caput	Reslice WT Caput 2.tif	60-360	43	0,1433	550-850	45	0,1500	1040-1340	39	0,1300	1510-1810	Yes
15.10.18	L	Cauda	Cauda 1b.tif	60-360	7	0,0233	560-860	9	0,0300	1060-1360	9	0,0300	1505-1805	Yes
24.10.18	M	Caput	Reslice WT 181024 Caput.tif	60-360	25	0,0833	560-860	26	0,0867	1060-1360	31	0,1033	1505-1805	Yes
24.10.18	M	Cauda	nicht auswertbar	60-360	0	0,0000	560-860	0	0,0000	1060-1360	0	0,0000	1510-1810	Yes
26.10.18	N	Caput	Reslice 181026 WT Caput 1.tif	60-360	32	0,1067	560-860	34	0,1133	1060-1360	38	0,1267	1505-1805	Yes
26.10.18	N	Cauda	Reslice of Tier N 181026 Cauda 2.tif	60-360	3	0,0100	560-860	4	0,0133	1060-1360	5	0,0167	1580-1880	Yes
09.11.18	O	Caput	Reslice of Tier N 181109 WT Caput.tif	60-360	41	0,1367	560-860	44	0,1467	1060-1360	42	0,1400	1505-1805	Yes
09.11.18	O	Cauda	nicht auswertbar	60-360	0	0,0000	560-860	0	0,0000	1060-1360	0	0,0000	1505-1805	Yes
05.03.18	Q	Caput	Reslice Tier Q of 190305.tif	60-360	22	0,0733	560-860	26	0,0867	1060-1360	34	0,1133	1505-1805	Yes
05.03.18	Q	Cauda	Reslice Tier Q of 190305 Cauda2.tif	60-360	6	0,0200	560-860	5	0,0167	1060-1360	7	0,0233	1505-1805	Yes
19.03.18	W	Caput	Reslice Tier W of 190319 Caput 1b.tif	60-360	27	0,0900	560-860	30	0,1000	990-1290	33	0,1100	1505-1805	Yes
19.03.18	W	Cauda	Reslice Tier W of 190319 Cauda1a.tif	60-360	16	0,0533	560-860	16	0,0533	1060-1360	16	0,0533	1505-1805	Yes
20.01.19	AA	Caput	Reslice of CapNH1	60-360	30	0,1000	560-860	32	0,1067	1060-1360	38	0,1267	1505-1805	Yes
20.01.19	AA	Cauda	Reslice of CauNH1	60-360	6	0,0200	560-860	2	0,0067	1060-1360	15	0,0500	1505-1805	Yes
03.03.19	AC	Caput	Reslice of CapNH2	60-360	9	0,0300	560-860	11	0,0367	1060-1360	17	0,0567	1505-1805	Yes
03.03.19	AC	Cauda	Reslice of CauNH2	60-360	17	0,0567	560-860	21	0,0700	1060-1360	26	0,0867	1505-1805	Yes
06.03.19	AD	Caput	Reslice of CapNH2	60-360	5	0,0167	560-860	6	0,0200	1060-1360	18	0,0600	1505-1805	Yes
06.03.19	AD	Cauda	Reslice of CapNH2	60-360	3	0,0100	560-860	0	0,0000	1060-1360	6	0,0200	1505-1805	Yes
08.03.19	AE	Caput	Resclice of CapNH1b	60-360	5	0,0167	560-860	15	0,0500	1060-1360	30	0,1000	1505-1805	Yes
08.03.19	AE	Cauda	Resclice of CapNH1b	60-360	12	0,0400	560-860	5	0,0167	1060-1360	17	0,0567	1505-1805	Yes

Intentionally left blank

8.7 Normal distribution tests

Table 8-3: Normal distribution tests

	WT caput			Trpm5 KO caput			WT cauda			Trpm5 KO cauda		
	0	10 µM	100 µM	0	10 µM	100 µM	0	10 µM	300 µM	0	10 µM	100 µM
Test for normal distribution												
D'Agostino & Pearson test												
K2	0,7418	1,83	3,396	4,387	1,795	1,712	3,451	2,624	0,7462	0,3256	0,557	0,2096
P value	0,6901	0,4006	0,183	0,1115	0,4075	0,4249	0,1781	0,2693	0,6886	0,8498	0,7569	0,9005
Passed normality test (alpha=0,05)?	Yes	Yes	Yes	Yes	Yes	Yes	Yes	Yes	Yes	Yes	Yes	Yes
P value summary	ns	ns	ns	ns	ns	ns	ns	ns	ns	ns	ns	ns
Shapiro-Wilk test												
W	0,8952	0,9094	0,9097	0,8919	0,9274	0,9297	0,9009	0,9255	0,9263	0,9022	0,9091	0,9445
P value	0,0805	0,1327	0,134	0,1036	0,3146	0,3379	0,1375	0,2977	0,3047	0,2314	0,2751	0,6035
Passed normality test (alpha=0,05)?	Yes	Yes	Yes	Yes	Yes	Yes	Yes	Yes	Yes	Yes	Yes	Yes
P value summary	ns	ns	ns	ns	ns	ns	ns	ns	ns	ns	ns	ns
Kolmogorov-Smirnov test												
KS distance	0,2016	0,1589	0,2187	0,1535	0,143	0,1432	0,1803	0,1756	0,1397	0,1842	0,1468	0,1387
P value	>0,1000	>0,1000	0,0518	>0,1000	>0,1000	>0,1000	>0,1000	>0,1000	>0,1000	>0,1000	>0,1000	>0,1000
Passed normality test (alpha=0,05)?	Yes	Yes	Yes	Yes	Yes	Yes	Yes	Yes	Yes	Yes	Yes	Yes
P value summary	ns	ns	ns	ns	ns	ns	ns	ns	ns	ns	ns	ns
Number of values	15	15	15	13	13	13	13	13	13	10	10	10

Intentionally left blank

8.8 Data: ANOVA results

Table 8-4: ANOVA results WT ms caput

Repeated measures one-way ANOVA - ANOVA results
WT ms epididymis caput - Data

ANOVA table	SS	DF	MS	F (DFn, DFd)	P value
Treatment (between columns)	0,0043	2	0,002137	F (1,578, 22,09) = 9,985	P=0,0016
Individual (between rows)	0,0579	14	0,004139	F (14, 28) = 19,34	P<0,0001
Residual (random)	0,0060	28	0,000214		
Total	0,0682	44			

Table 8-5: ANOVA results WT ms cauda

Repeated measures one-way ANOVA - ANOVA results
WT ms epididymis cauda - Data

ANOVA table	SS	DF	MS	F (DFn, DFd)	P value
Treatment (between columns)	0,0013	2	0,000673	F (1,702, 20,43) = 8,069	P=0,0037
Individual (between rows)	0,0146	12	0,001218	F (12, 24) = 14,60	P<0,0001
Residual (random)	0,0020	24	0,000083		
Total	0,0180	38			

Table 8-6: ANOVA results Trpm5 KO ms caput

Repeated measures one-way ANOVA - ANOVA results
Trpm5 KO ms epididymis caput - Data

ANOVA table	SS	DF	MS	F (DFn, DFd)	P value
Treatment (between columns)	0,0006	2	0,000305	F (1,368, 16,42) = 1,405	P=0,2645
Individual (between rows)	0,0174	12	0,001450	F (12, 24) = 6,685	P<0,0001
Residual (random)	0,0052	24	0,000217		
Total	0,0232	38			

Table 8-7: ANOVA results Trpm5 KO ms cauda

Repeated measures one-way ANOVA - ANOVA results
Trpm5 KO ms epididymis cauda - Data

ANOVA table	SS	DF	MS	F (DFn, DFd)	P value
Treatment (between columns)	0,0005	2	0,000251	F (1,531, 13,78) = 2,844	P=0,1022
Individual (between rows)	0,0427	9	0,004747	F (9, 18) = 53,90	P<0,0001
Residual (random)	0,0016	18	0,000088		
Total	0,0448	29			

8.9 Critical values of F for the 0.05 significance level

How to use this table:

There are two tables here. The first one gives critical values of F at the p = 0.05 level of significance.
The second table gives critical values of F at the p = 0.01 level of significance.
1. Obtain your F-ratio. This has (x,y) degrees of freedom associated with it.
2. Go along x columns, and down y rows. The point of intersection is your critical F-ratio.
3. If your obtained value of F is equal to or larger than this critical F-value, then your result is significant at that level of probability.
An example: I obtain an F ratio of 3.96 with (2, 24) degrees of freedom.
I go along 2 columns and down 24 rows. The critical value of F is 3.40. My obtained F-ratio is larger than this, and so I conclude that my obtained F-ratio is likely to occur by chance with a p<.05.

Critical values of F for the 0.05 significance level:

	1	2	3	4	5	6	7	8	9	10
1	161.45	199.50	215.71	224.58	230.16	233.99	236.77	238.88	240.54	241.88
2	18.51	19.00	19.16	19.25	19.30	19.33	19.35	19.37	19.39	19.40
3	10.13	9.55	9.28	9.12	9.01	8.94	8.89	8.85	8.81	8.79
4	7.71	6.94	6.59	6.39	6.26	6.16	6.09	6.04	6.00	5.96
5	6.61	5.79	5.41	5.19	5.05	4.95	4.88	4.82	4.77	4.74
6	5.99	5.14	4.76	4.53	4.39	4.28	4.21	4.15	4.10	4.06
7	5.59	4.74	4.35	4.12	3.97	3.87	3.79	3.73	3.68	3.64
8	5.32	4.46	4.07	3.84	3.69	3.58	3.50	3.44	3.39	3.35
9	5.12	4.26	3.86	3.63	3.48	3.37	3.29	3.23	3.18	3.14
10	4.97	4.10	3.71	3.48	3.33	3.22	3.14	3.07	3.02	2.98
11	4.84	3.98	3.59	3.36	3.20	3.10	3.01	2.95	2.90	2.85
12	4.75	3.89	3.49	3.26	3.11	3.00	2.91	2.85	2.80	2.75
13	4.67	3.81	3.41	3.18	3.03	2.92	2.83	2.77	2.71	2.67
14	4.60	3.74	3.34	3.11	2.96	2.85	2.76	2.70	2.65	2.60
15	4.54	3.68	3.29	3.06	2.90	2.79	2.71	2.64	2.59	2.54
16	4.49	3.63	3.24	3.01	2.85	2.74	2.66	2.59	2.54	2.49
17	4.45	3.59	3.20	2.97	2.81	2.70	2.61	2.55	2.49	2.45
18	4.41	3.56	3.16	2.93	2.77	2.66	2.58	2.51	2.46	2.41
19	4.38	3.52	3.13	2.90	2.74	2.63	2.54	2.48	2.42	2.38
20	4.35	3.49	3.10	2.87	2.71	2.60	2.51	2.45	2.39	2.35
21	4.33	3.47	3.07	2.84	2.69	2.57	2.49	2.42	2.37	2.32
22	4.30	3.44	3.05	2.82	2.66	2.55	2.46	2.40	2.34	2.30
23	4.28	3.42	3.03	2.80	2.64	2.53	2.44	2.38	2.32	2.28
24	4.26	3.40	3.01	2.78	2.62	2.51	2.42	2.36	2.30	2.26
25	4.24	3.39	2.99	2.76	2.60	2.49	2.41	2.34	2.28	2.24
26	4.23	3.37	2.98	2.74	2.59	2.47	2.39	2.32	2.27	2.22
27	4.21	3.35	2.96	2.73	2.57	2.46	2.37	2.31	2.25	2.20
28	4.20	3.34	2.95	2.71	2.56	2.45	2.36	2.29	2.24	2.19
29	4.18	3.33	2.93	2.70	2.55	2.43	2.35	2.28	2.22	2.18
30	4.17	3.32	2.92	2.69	2.53	2.42	2.33	2.27	2.21	2.17
31	4.16	3.31	2.91	2.68	2.52	2.41	2.32	2.26	2.20	2.15
32	4.15	3.30	2.90	2.67	2.51	2.40	2.31	2.24	2.19	2.14
33	4.14	3.29	2.89	2.66	2.50	2.39	2.30	2.24	2.18	2.13
34	4.13	3.28	2.88	2.65	2.49	2.38	2.29	2.23	2.17	2.12
35	4.12	3.27	2.87	2.64	2.49	2.37	2.29	2.22	2.16	2.11

Figure 8-3; Critical values of F for the 0.05 significance level

Source:https://www.google.com/url?sa=t&source=web&rct=j&opi=89978449&url=http://users.sussex.ac.uk/~grahamh/RM1web/F-ratio%2520table%25202005.pdf&ved=2ahUKEwiYgd6v3b6KAxW977sIHSQyGR8QFnoECBcQAQ&usg=AOvVaw18imAGfwIFXfmKc5qW1thq

8.10 Explanation of the statistical terms

ANOVA:

An ANOVA (Analysis of Variance) has to be used if 3 or more effects (comparison of spontaneous contraction with application of 10µM and 100µM denatonium) should be analyzed whereas a t-test can only be used for up to two effects. If a t-test would be applied, the probability of error would be beyond 40%. As mentioned above, the t-test is not possible as this experiment consists of more than two random samples. The ANOVA computes the differences in the means of each group of effects. It also computes the effect of the mean within the groups. That means that the ANOVA checks wheth-

er there are statistical differences between the mean values of a factor (e.g. wild type mice epididymis caput) with more than two levels, i.e. effects (comparison of spontaneous contraction with application of 10µM and 100µM denatonium).

Repeated measures:

In general, experimental designs with repeated measurements are considered a very efficient type of research. In such designs, the same test subjects are usually measured several times. The idea behind this is simple: by keeping the subjects the same, the variance can be better estimated (as the error variance is minimized using the same subject) and attribute possible effects (comparison of spontaneous contraction with application of 10µM and 100µM denatonium). In other words, the subjects are their own “control group”. As a result, repeated measures designs also generally have higher statistical power.

One-way

That means that only one effect is analyzed. In this study, the analysis focuses on the effect of denatonium (DNT) on the contraction pattern of smooth muscles.

The repeated measures one-way ANOVA has to fulfil the following minimum requirements in order to be meaningful:

1. Data has to be correlated, i.e. been collected from the same subject (e.g. wild type mouse A caput).
2. The dependent variable is at least interval scaled i.e. frequency of contractions of the smooth muscles.
3. Data has to measure at least 3 effects (comparison of spontaneous contraction with application of 10µM and 100µM denatonium).
4. Data has to be normal distributed. All data of this research is normal distributed.
5. Data should not have any outliers. There are no outliers within the data.

6. Sphericity should be given if there are no variances between columns. As per recommendation by GraphPad, sphericity had not been assumed, as the variances differ between columns. That means that there should always be a violation of as the variances always differ between columns. Therefore, the Geisser-Greenhouse's epsilon was computed. In summary, the Geisser-Greenhouse's epsilon leads to a higher P-value, thereby introducing a degree of statistical protection into the calculations. This allows a conservative interpretation of the p-values and thus, supports a robust statement about the results. Specially, for the WT mouse, the Geisser-Greenhouse's epsilon demonstrates almost no violation which supports the results of this study.

Furthermore, the statistical significance is corroborated by a comparison of the F-ratios, which take a 5% confidence interval into account (see Table 4-8) with $F_{crit} < F$-

ratio for the wild type mice. F_{crit} is derived from the table shown in Figure 8-3.

Additionally, the F-value, which is the ratio between the variance within groups and the variance between groups, is displayed. A high F-value indicates that the variance be-tween groups is greater than the variance within groups. This indicates that there is a **statistically significant difference** between the group means.

Interpretation of graphs (e.g. Figure 4-8)

Graph A shows the p-values of each level/effect.

Graph B shows the “column means” of the 95% confidence interval (Tukey test). If a line strikes the x = 0 line, the effect is **not statistically significant**.

Graph C shows the “Differences” of within each level/effect. It allows only a rough estimate how homogenous the effects are.

Graph D shows the QQ Plot which confirms homoscedasticity (variance is similar between data points), i.e. shows that the scatter of the points around the straight

line in the vertical direction is constant. That indicates a normal distribution as computed with the normal distribution tests (see Table 8-3). In all cases the normal distribution of the data is confirmed (very similar auxiliary and correlation lines**).**

8.11 List of agreements

Below are the agreements/permissions to use figures from other sources:

1. Figure 1-2: This work is in the public domain in the United States because it was prepared by employees of the United States Federal Government or one of its agencies in the performance of their official duties and is therefore a work of the United States Government under Title 17, Chapter 1, Section 105 of the United States Code.
2. Figure 1-3: permission by email, date 11.11.2024
3. Figure 1-7: permission by email, date 13.11.2024
4. Figure 1-9: permission by email, date 13.11.2024

9 List of Literature

1. Abramowitz, J./Flockerzi, Veit/Nilius, B. (2007). Transient receptor potential (TRP) channels. Berlin/New York, Springer.

2. Amann, R. P./Howards, S. S. (1980). Daily Spermatozoal Production and Epididymal Spermatozoal Reserves of the Human Male. The Journal of urology 124 (2), 211–215. https://doi.org/10.1016/S0022-5347(17)55377-X.

3. Aumüller, Gerhard/Wurzinger, Laurenz J. (2010). Anatomie. 208 Tabellen. 2nd ed. Stuttgart, Thieme.

4. Avau, Bert/Rotondo, Alessandra/Thijs, Theo/Andrews, Christopher N./Janssen, Pieter/Tack, Jan/Depoortere, Inge (2015). Targeting extra-oral bitter taste receptors modulates gastrointestinal motility with effects on satiation. Scientific reports 5, 15985. https://doi.org/10.1038/srep15985.

5. Bachmanov, Alexander A./Bosak, Natalia P./Lin, Cailu/Matsumoto, Ichiro/Ohmoto, Makoto/Reed, Danielle R./Nelson, Theodore M. (2014). Genetics of taste receptors. Current pharmaceutical design 20 (16), 2669–2683. https://doi.org/10.2174/13816128113199990566.

6. Balemans, Dafne/Boeckxstaens, Guy E./Talavera, Karel/Wouters, Mira M. (2017). Transient receptor potential ion channel function in sensory transduction and cellular signaling cascades underlying visceral hypersensitivity. American journal of physiology. Gastrointestinal and liver physiology 312 (6), G635-G648. https://doi.org/10.1152/ajpgi.00401.2016.

7. Banik, Debarghya Dutta/Martin, Laura E./Freichel, Marc/Torregrossa, Ann-Marie/Medler, Kathryn F. (2018). TRPM4 and TRPM5 are both required for normal signaling in taste receptor cells. Proceedings of the National Academy of Sciences of the United States of America 115 (4), E772-E781. https://doi.org/10.1073/pnas.1718802115.

8. Bedford, J. M. (1967). Effects of duct ligation on the fertilizing ability of spermatozoa from different regions of the rabbit epididymis. The Journal of experimental zoology 166 (2), 271–281. https://doi.org/10.1002/jez.1401660210.

9. Bedford, J. M. (1994). The status and the state of the human epididymis. Human Reproduction 9 (11), 2187–2199. https://doi.org/10.1093/oxfordjournals.humrep.a138416.

10. Bezençon, C./Fürholz, A./Raymond, F./Mansourian, R./Métairon, S./Le Coutre, J./Damak, S. (2008). Murine intestinal cells expressing Trpm5 are mostly brush cells and express markers of neuronal and inflammatory cells. The Journal of comparative neurology 509 (5), 514–525. https://doi.org/10.1002/cne.21768.

11. Bezençon, Carole/Le Coutre, Johannes/Damak, Sami (2007). Taste-signaling proteins are coexpressed in solitary intestinal epithelial cells. Chem-

ical senses 32 (1), 41–49. https://doi.org/10.1093/chemse/bjl034.

12. Breton, Sylvie/Brown, Dennis (2013). Regulation of luminal acidification by the V-ATPase. Physiology (Bethesda, Md.) 28 (5), 318–329. https://doi.org/10.1152/physiol.00007.2013.

13. Carey, Ryan M./Workman, Alan D./Yan, Carol H./Chen, Bei/Adappa, Nithin D./Palmer, James N./Kennedy, David W./Lee, Robert J./Cohen, Noam A. (2017). Sinonasal T2R-mediated nitric oxide production in response to Bacillus cereus. American journal of rhinology & allergy 31 (4), 211–215. https://doi.org/10.2500/ajra.2017.31.4453.

14. Carr, D. W./Acott, T. S. (1984). Inhibition of bovine spermatozoa by caudal epididymal fluid: I. Studies of a sperm motility quiescence factor. Biology of Reproduction 30 (4), 913–925. https://doi.org/10.1095/biolreprod30.4.913.

15. Chandrakesan, Parthasarathy/May, Randal/Weygant, Nathaniel/Qu, Dongfeng/Berry, William L./Sureban, Sripathi M./Ali, Naushad/Rao,

Chinthalapally/Huycke, Mark/Bronze, Michael S./Houchen, Courtney W. (2016). Intestinal tuft cells regulate the ATM mediated DNA Damage response via Dclk1 dependent mechanism for crypt restitution following radiation injury. Scientific reports 6, 1. https://doi.org/10.1038/srep37667.

16. Chandrashekar, Jayaram/Mueller, Ken L./Hoon, Mark A./Adler, Elliot/Feng, Luxin/Guo, Wei/Zuker, Charles S./Ryba, Nicholas J.P (2000). T2Rs Function as Bitter Taste Receptors. Cell 100 (6), 703–711. https://doi.org/10.1016/S0092-8674(00)80706-0.

17. Chaudhari, Nirupa/Roper, Stephen D. (2010). The cell biology of taste. The Journal of cell biology 190 (3), 285–296. https://doi.org/10.1083/JCB.201003144.

18. Clapham, David E./Julius, David/Montell, Craig/Schultz, Günter (2005). International Union of Pharmacology. XLIX. Nomenclature and structure-function relationships of transient receptor po-

tential channels. Pharmacological reviews 57 (4), 427–450. https://doi.org/10.1124/pr.57.4.6.

19. Clapp, Tod R./Stone, Leslie M./Margolskee, Robert F./Kinnamon, Sue C. (2001). Immunocytochemical evidence for co-expression of Type III IP3 receptor with signaling components of bitter taste transduction. BMC neuroscience 2, 6. https://doi.org/10.1186/1471-2202-2-6.

20. Cornwall, Gail A. (2009). New insights into epididymal biology and function. Human Reproduction Update 15 (2), 213–227. https://doi.org/10.1093/humupd/dmn055.

21. D'Agostino, Pearson (1973). Tests for departure from normality. Empirical results for the distribution of b2 and √b1.

22. Damak, Sami/Rong, Minqing/Yasumatsu, Keiko/Kokrashvili, Zaza/Pérez, Cristian A./Shigemura, Noriatsu/Yoshida, Ryusuke/Mosinger, Bedrich/Glendinning, John I./Ninomiya, Yuzo/Margolskee, Robert F. (2006). Trpm5 null mice respond to bitter, sweet, and umami compounds.

Chemical senses 31 (3), 253–264. https://doi.org/10.1093/chemse/bjj027.

23. Deckmann, Klaus/Filipski, Katharina/Krasteva-Christ, Gabriela/Fronius, Martin/Althaus, Mike/Rafiq, Amir/Papadakis, Tamara/Renno, Liane/Jurastow, Innokentij/Wessels, Lars/Wolff, Miriam/Schütz, Burkhard/Weihe, Eberhard/Chubanov, Vladimir/Gudermann, Thomas/Klein, Jochen/Bschleipfer, Thomas/Kummer, Wolfgang (2014). Bitter triggers acetylcholine release from polymodal urethral chemosensory cells and bladder reflexes. Proceedings of the National Academy of Sciences of the United States of America 111 (22), 8287–8292. https://doi.org/10.1073/pnas.1402436111.

24. Deckmann, Klaus/Kummer, Wolfgang (2016). Chemosensory epithelial cells in the urethra: sentinels of the urinary tract. Histochemistry and cell biology 146 (6), 673–683. https://doi.org/10.1007/s00418-016-1504-x.

25. Deckmann, Klaus/Rafiq, Amir/Erdmann, Christian/Illig, Christian/Durschnabel, Melanie/Wess, Jürgen/Weidner, Wolfgang/Bschleipfer, Thomas/Kummer, Wolfgang (2018). Muscarinic receptors 2 and 5 regulate bitter response of urethral brush cells via negative feedback. FASEB journal : official publication of the Federation of American Societies for Experimental Biology 32 (6), 2903–2910. https://doi.org/10.1096/fj.201700582R.

26. Domeniconi, Raquel F./Souza, Ana Cláudia Ferreira/Xu, Bingfang/Washington, Angela M./Hinton, Barry T. (2016). Is the Epididymis a Series of Organs Placed Side By Side? Biology of Reproduction 95 (1), 10. https://doi.org/10.1095/biolreprod.116.138768.

27. Dorscht, Ludmilla (2020). Non-neuronale cholinerge chemosensorische Zellen im Nebenhodenepithel. Doctoral thesis. Giessen, JLU-Giessen.

28. Elfgen, V./Mietens, A./Mewe, M./Hau, T./Middendorff, R. (2018). Contractility of the epi-

didymal duct: function, regulation and potential drug effects. Reproduction 156 (4), R125-R141. https://doi.org/10.1530/REP-17-0754.

29. Fehr, Johanna/Meyer, Dorke/Widmayer, Patricia/Borth, Heike Claudia/Ackermann, Frauke/Wilhelm, Beate/Gudermann, Thomas/Boekhoff, Ingrid (2007). Expression of the G-protein alpha-subunit gustducin in mammalian spermatozoa. Journal of comparative physiology. A, Neuroethology, sensory, neural, and behavioral physiology 193 (1), 21–34. https://doi.org/10.1007/s00359-006-0168-8.

30. Finger, Thomas E./Böttger, Bärbel/Hansen, Anne/Anderson, Karl T./Alimohammadi, Hessamedin/Silver, Wayne L. (2003). Solitary chemoreceptor cells in the nasal cavity serve as sentinels of respiration. Proceedings of the National Academy of Sciences of the United States of America 100 (15), 8981–8986. https://doi.org/10.1073/pnas.1531172100.

31. Foster, Simon R./Blank, Kristina/See Hoe, Louise E./Behrens, Maik/Meyerhof, Wolfgang/Peart, Jason N./Thomas, Walter G. (2014). Bitter taste receptor agonists elicit G-protein-dependent negative inotropy in the murine heart. The FASEB Journal 28 (10), 4497–4508. https://doi.org/10.1096/fj.14.256305.

32. Garcia, R. L./Schilling, W. P. (1997). Differential expression of mammalian TRP homologues across tissues and cell lines. Biochemical and biophysical research communications 239 (1), 279–283. https://doi.org/10.1006/bbrc.1997.7458.

33. Gerbe, François/van Es, Johan H./Makrini, Leila/Brulin, Bénédicte/Mellitzer, Georg/Robine, Sylvie/Romagnolo, Béatrice/Shroyer, Noah F./Bourgaux, Jean-François/Pignodel, Christine/Clevers, Hans/Jay, Philippe (2011). Distinct ATOH1 and Neurog3 requirements define tuft cells as a new secretory cell type in the intestinal epithelium. The Journal of cell biology 192 (5), 767–780. https://doi.org/10.1083/jcb.201010127.

34. GraphPad (2020). GraphPad Prism 8 Statistics Guide - Choosing a normality test. Available online at https://www.graphpad.com/guides/prism/8/statistics/stat_choosing_a_normality_test.htm (accessed 9/2/2020).

35. GraphPad (2020). GraphPad Prism 8 Statistics Guide - Tukey and Dunnett methods. Available online at https://www.graphpad.com/guides/prism/8/statistics/stat_the_methods_of_tukey_and_dunne.htm (accessed 9/2/2020).

36. GraphPad (2023). Prism Academy. Available online at https://www.graphpad.com/prism-academy.

37. Guinamard, Romain/Sallé, Laurent/Simard, Christophe (2011). The non-selective monovalent cationic channels TRPM4 and TRPM5. Advances in experimental medicine and biology 704, 147–171. https://doi.org/10.1007/978-94-007-0265-3_8.

38. Gulbransen, Brian D./Clapp, Tod R./Finger, Thomas E./Kinnamon, Sue C. (2008). Nasal solitary chemoreceptor cell responses to bitter and trigeminal stimulants in vitro. Journal of neurophysiology 99 (6), 2929–2937. https://doi.org/10.1152/jn.00066.2008.

39. Hantute-Ghesquier, Aline/Haustrate, Aurélien/Prevarskaya, Natalia/Lehen'kyi, V'yacheslav (2018). TRPM Family Channels in Cancer. Pharmaceuticals (Basel, Switzerland) 11 (2). https://doi.org/10.3390/ph11020058.

40. Hinton, Barry T./Galdamez, Maureen M./Sutherland, Ann/Bomgardner, Daniela/Xu, Bingfang/Abdel-Fattah, Rana/Yang, Ling (2011). How do you get six meters of epididymis inside a human scrotum? Journal of andrology 32 (6), 558–564. https://doi.org/10.2164/jandrol.111.013029.

41. Höfer, D./Püschel, B./Drenckhahn, D. (1996). Taste receptor-like cells in the rat gut identified by expression of alpha-gustducin. Proceedings of the National Academy of Sciences of the United

States of America 93 (13), 6631–6634. https://doi.org/10.1073/pnas.93.13.6631.

42. Hoffmann, J. G./Langner, C./Rüschoff, J./Melchior, H. (2000). Das adenomatoide Leiomyom des Nebenhodens — ein seltener gutartiger Tumor. Der Urologe B 40 (3), 251–254. https://doi.org/10.1007/s001310050401.

43. Hofmann, Thomas/Chubanov, Vladimir/Gudermann, Thomas/Montell, Craig (2003). TRPM5 Is a Voltage-Modulated and Ca2+-Activated Monovalent Selective Cation Channel. Current Biology 13 (13), 1153–1158. https://doi.org/10.1016/S0960-9822(03)00431-7.

44. Hollenhorst, Monika I./Krasteva-Christ, Gabriela (2023). Chemosensory cells in the respiratory tract as crucial regulators of innate immune responses. The Journal of Physiology 601 (9), 1555–1572. https://doi.org/10.1113/JP282307.

45. Huang, L./Shanker, Y. G./Dubauskaite, J./Zheng, J. Z./Yan, W./Rosenzweig, S./Spielman, A. I./Max, M./Margolskee, R. F. (1999). Ggamma13 colocal-

izes with gustducin in taste receptor cells and mediates IP3 responses to bitter denatonium. Nature neuroscience 2 (12), 1055–1062. https://doi.org/10.1038/15981.

46. human gene nomenclature (Hrsg.) (2019). TRPM5 gene symbol report | HUGO Gene Nomenclature Committee. Available online at https://www.genenames.org/data/gene-symbol-report/#!/hgnc_id/HGNC:14323 (accessed 5/9/2019).

47. Jelinsky, Scott A./Turner, Terry T./Bang, Hyun J./Finger, Joshua N./Solarz, Mark K./Wilson, Ewa/Brown, Eugene L./Kopf, Gregory S./Johnston, Daniel S. (2007). The rat epididymal transcriptome: comparison of segmental gene expression in the rat and mouse epididymides. Biology of Reproduction 76 (4), 561–570. https://doi.org/10.1095/biolreprod.106.057323.

48. Jhang, Jia-Fong/Kuo, Hann-Chorng (2017). Recent advances in recurrent urinary tract infection from pathogenesis and biomarkers to prevention.

Tzu-Chi Medical Journal 29 (3), 131–137. https://doi.org/10.4103/tcmj.tcmj_53_17.

49. Jones, R. C./Clulow, J. (1987). Regulation of the elemental composition of the epididymal fluids in the tammar, Macropus eugenii. Journal of reproduction and fertility 81 (2), 583–590. https://doi.org/10.1530/jrf.0.0810583.

50. Kaji, Izumi/Karaki, Shin-ichiro/Fukami, Yasuyuki/Terasaki, Masaki/Kuwahara, Atsukazu (2009). Secretory effects of a luminal bitter tastant and expressions of bitter taste receptors, T2Rs, in the human and rat large intestine. American journal of physiology. Gastrointestinal and liver physiology 296 (5), G971-81. https://doi.org/10.1152/ajpgi.90514.2008.

51. Kanehisa Laboratory in Kyoto University (2022). Taste transduction. Available online at https://www.genome.jp/dbget-bin/www_bget?hsa04742.

52. Kanehisa, Minoru/Sato, Yoko/Kawashima, Masayuki (2022). KEGG mapping tools for uncover-

ing hidden features in biological data. Protein science : a publication of the Protein Society 31 (1), 47–53. https://doi.org/10.1002/pro.4172.

53. Kaske, Silke/Krasteva, Gabriele/König, Peter/Kummer, Wolfgang/Hofmann, Thomas/Gudermann, Thomas/Chubanov, Vladimir (2007). TRPM5, a taste-signaling transient receptor potential ion-channel, is a ubiquitous signaling component in chemosensory cells. BMC neuroscience 8, 49. https://doi.org/10.1186/1471-2202-8-49.

54. Konopka, R. J./Benzer, S. (1971). Clock mutants of Drosophila melanogaster. Proceedings of the National Academy of Sciences of the United States of America 68 (9), 2112–2116. https://doi.org/10.1073/pnas.68.9.2112.

55. Krasteva, G./Canning, B. J./Papadakis, T./Kummer, W. (2012). Cholinergic brush cells in the trachea mediate respiratory responses to quorum sensing molecules. Life sciences 91 (21-

22), 992–996. https://doi.org/10.1016/j.lfs.2012.06.014.

56. Krasteva, Gabriela/Canning, Brendan J./Hartmann, Petra/Veres, Tibor Z./Papadakis, Tamara/Mühlfeld, Christian/Schliecker, Kirstin/Tallini, Yvonne N./Braun, Armin/Hackstein, Holger/Baal, Nelli/Weihe, Eberhard/Schütz, Burkhard/Kotlikoff, Michael/Ibanez-Tallon, Ines/Kummer, Wolfgang (2011). Cholinergic chemosensory cells in the trachea regulate breathing. Proceedings of the National Academy of Sciences 108 (23), 9478–9483. https://doi.org/10.1073/pnas.1019418108.

57. Krasteva-Christ, G./Soultanova, A./Schütz, B./Papadakis, T./Weiss, C./Deckmann, K./Chubanov, V./Gudermann, T./Voigt, A./Meyerhof, W./Boehm, U./Weihe, E./Kummer, W. (2015). Identification of cholinergic chemosensory cells in mouse tracheal and laryngeal glandular ducts. International immunopharmacology 29 (1), 158–165. https://doi.org/10.1016/j.intimp.2015.05.028.

58. Kügler, Robert/Mietens, Andrea/Seidensticker, Mathias/Tasch, Sabine/Wagenlehner, Florian M./Kaschtanow, Andre/Tjahjono, Yudy/Tomczyk, Claudia U./Beyer, Daniela/Risbridger, Gail P./Exintaris, Betty/Ellem, Stuart J./Middendorff, Ralf (2018). Novel imaging of the prostate reveals spontaneous gland contraction and excretory duct quiescence together with different drug effects. The FASEB Journal 32 (3), 1130–1138. https://doi.org/10.1096/fj.201700430R.

59. Kummer, Wolfgang/Deckmann, Klaus (2017). Brush cells, the newly identified gatekeepers of the urinary tract. Current opinion in urology 27 (2), 85–92. https://doi.org/10.1097/MOU.0000000000000361.

60. Lee, Sangseok/Lee, Dong Kyu (2018). What is the proper way to apply the multiple comparison test? Korean journal of anesthesiology 71 (5), 353–360. https://doi.org/10.4097/kja.d.18.00242.

61. Lemons, Kayla/Fu, Ziying/Aoudé, Imad/Ogura, Tatsuya/Sun, Julianna/Chang, Justin/Mbonu,

Kenechukwu/Matsumoto, Ichiro/Arakawa, Hiroyuki/Lin, Weihong (2017). Lack of TRPM5-Expressing Microvillous Cells in Mouse Main Olfactory Epithelium Leads to Impaired Odor-Evoked Responses and Olfactory-Guided Behavior in a Challenging Chemical Environment. eNeuro 4 (3). https://doi.org/10.1523/ENEURO.0135-17.2017.

62. Leung, G. P. H./Cheung, K. H./Leung, C. T./Tsang, M. W./Wong, P. Y. D. (2004). Regulation of epididymal principal cell functions by basal cells: role of transient receptor potential (Trp) proteins and cyclooxygenase-1 (COX-1). Molecular and cellular endocrinology 216 (1-2), 5–13. https://doi.org/10.1016/j.mce.2003.10.077.

63. Leung, P. S./Chan, H. C./Chung, Y. W./Wong, T. P./Wong, P. Y. (1998). The role of local angiotensins and prostaglandins in the control of anion secretion by the rat epididymis. Journal of reproduction and fertility. Supplement 53, 15–22.

64. Li, Feng (2013). Taste perception: from the tongue to the testis. Molecular Human Reproduction 19

(6), 349–360. https://doi.org/10.1093/molehr/gat009.

65. Liman, E. R. (2007a). TRPM5 and taste transduction. Handbook of experimental pharmacology (179), 287–298. https://doi.org/10.1007/978-3-540-34891-7_17.

66. Liman, Emily R. (2007b). TRP Ion Channel Function in Sensory Transduction and Cellular Signaling Cascades. The Ca2+-Activated TRP Channels: TRPM4 and TRPM5.

67. Liu, Dan/Liman, Emily R. (2003). Intracellular Ca2+ and the phospholipid PIP2 regulate the taste transduction ion channel TRPM5. Proceedings of the National Academy of Sciences of the United States of America 100 (25), 15160–15165. https://doi.org/10.1073/pnas.2334159100.

68. Liu, Pin/Shah, Bhavik P./Croasdell, Stephanie/Gilbertson, Timothy A. (2011). Transient receptor potential channel type M5 is essential for fat taste. The Journal of Neuroscience 31 (23), 8634–8642.

https://doi.org/10.1523/JNEUROSCI.6273-10.2011.

69. Lossow, Kristina/Hübner, Sandra/Roudnitzky, Natacha/Slack, Jay P./Pollastro, Federica/Behrens, Maik/Meyerhof, Wolfgang (2016). Comprehensive Analysis of Mouse Bitter Taste Receptors Reveals Different Molecular Receptive Ranges for Orthologous Receptors in Mice and Humans. The Journal of biological chemistry 291 (29), 15358–15377. https://doi.org/10.1074/jbc.M116.718544.

70. Lu, Ping/Zhang, Cheng-Hai/Lifshitz, Lawrence M./ZhuGe, Ronghua (2017). Extraoral bitter taste receptors in health and disease. The Journal of general physiology 149 (2), 181–197. https://doi.org/10.1085/jgp.201611637.

71. Mandon, Marion/Hermo, Louis/Cyr, Daniel G. (2015). Isolated Rat Epididymal Basal Cells Share Common Properties with Adult Stem Cells. Biology of Reproduction 93 (5), 115. https://doi.org/10.1095/biolreprod.115.133967.

72. Matos, Leandro Luongo de/Trufelli, Damila Cristina/Matos, Maria Graciela Luongo de/da Silva Pinhal, Maria Aparecida (2010). Immunohistochemistry as an important tool in biomarkers detection and clinical practice. Biomarker Insights 5, 9–20. https://doi.org/10.4137/bmi.s2185.

73. matthey.com (2017). The world's worst bitter: discovered, 'brewed' and tested in Scotland.

74. McLaughlin, S. K./McKinnon, P. J./Robichon, A./Spickofsky, N./Margolskee, R. F. (1993). Gustducin and transducin: a tale of two G proteins. Ciba Foundation symposium 179, 186-96; discussion 196-200. https://doi.org/10.1002/9780470514511.ch12.

75. Mewe, Marco/Bauer, Christiane K./Müller, Dieter/Middendorff, Ralf (2006a). Regulation of spontaneous contractile activity in the bovine epididymal duct by cyclic guanosine 5'-monophosphate-dependent pathways. Endocrinology 147 (4), 2051–2062. https://doi.org/10.1210/en.2005-1324.

76. Mewe, Marco/Bauer, Christiane K./Schwarz, Jürgen R./Middendorff, Ralf (2006b). Mechanisms regulating spontaneous contractions in the bovine epididymal duct. Biology of Reproduction 75 (4), 651–659. https://doi.org/10.1095/biolreprod.106.054577.

77. Meyerhof, Wolfgang/Batram, Claudia/Kuhn, Christina/Brockhoff, Anne/Chudoba, Elke/Bufe, Bernd/Appendino, Giovanni/Behrens, Maik (2010). The molecular receptive ranges of human TAS2R bitter taste receptors. Chemical Senses 35 (2), 157–170. https://doi.org/10.1093/chemse/bjp092.

78. Michel, Vera/Pilatz, Adrian/Hedger, Mark P./Meinhardt, Andreas (2015). Epididymitis: revelations at the convergence of clinical and basic sciences. Asian journal of andrology 17 (5), 756–763. https://doi.org/10.4103/1008-682X.155770.

79. Middelhoff, Moritz/Westphalen, C. Benedikt/Hayakawa, Yoku/Yan, Kelley S./Gershon, Michael D./Wang, Timothy C./Quante, Michael (2017). Dclk1-expressing tuft cells: critical modula-

tors of the intestinal niche? American journal of physiology. Gastrointestinal and liver physiology 313 (4), G285-G299. https://doi.org/10.1152/ajpgi.00073.2017.

80. Mietens, Andrea/Tasch, Sabine/Stammler, Angelika/Konrad, Lutz/Feuerstacke, Caroline/Middendorff, Ralf (2014). Time-lapse imaging as a tool to investigate contractility of the epididymal duct--effects of cGMP signaling. PloS one 9 (3), e92603. https://doi.org/10.1371/journal.pone.0092603.

81. National Center of Biotechnology Information (2020). Denatomium benzoate. Available online at https://pubchem.ncbi.nlm.nih.gov/.

82. Nickel, J. Curtis (2005). Management of urinary tract infections: historical perspective and current strategies: Part 1--Before antibiotics. The Journal of urology 173 (1), 21–26. https://doi.org/10.1097/01.ju.0000141496.59533.b2.

83. Nickel, J. Curtis (2019). Review Articles | Journal of Urology. Available online at https://www.auajournals.org/doi/10.1097/01.ju.0000141496.59533.b2 (accessed 9/14/2019).

84. Ogura, Tatsuya/Mackay-Sim, Alan/Kinnamon, Sue C. (1997). Bitter Taste Transduction of Denatonium in the Mudpuppy Necturus maculosus. The Journal of Neuroscience 17 (10), 3580–3587. https://doi.org/10.1523/JNEUROSCI.17-10-03580.1997.

85. Ostertagova, Eva/Ostertag, Oskar (2013). Methodology and Application of One-way ANOVA.

86. Pérez, Cristian A./Huang, Liquan/Rong, Minqing/Kozak, J. Ashot/Preuss, Axel K./Zhang, Hailin/Max, Marianna/Margolskee, Robert F. (2002). A transient receptor potential channel expressed in taste receptor cells. Nature neuroscience 5 (11), 1169–1176. https://doi.org/10.1038/nn952.

87. Perniss, Alexander/Boonen, Brett/Tonack, Sarah/Thiel, Moritz/Poharkar, Krupali/Alnouri, Mohamad Wessam/Keshavarz, Maryam/Papadakis,

Tamara/Wiegand, Silke/Pfeil, Uwe/Richter, Katrin/Althaus, Mike/Oberwinkler, Johannes/Schütz, Burkhard/Boehm, Ulrich/Offermanns, Stefan/Leinders-Zufall, Trese/Zufall, Frank/Kummer, Wolfgang (2023). A succinate/SUCNR1-brush cell defense program in the tracheal epithelium. Science advances 9 (31), eadg8842. https://doi.org/10.1126/sciadv.adg8842.

88. Perniss, Alexander/Liu, Shuya/Boonen, Brett/Keshavarz, Maryam/Ruppert, Anna-Lena/Timm, Thomas/Pfeil, Uwe/Soultanova, Aichurek/Kusumakshi, Soumya/Delventhal, Lucas/Aydin, Öznur/Pyrski, Martina/Deckmann, Klaus/Hain, Torsten/Schmidt, Nadine/Ewers, Christa/Günther, Andreas/Lochnit, Günter/Chubanov, Vladimir/Gudermann, Thomas/Oberwinkler, Johannes/Klein, Jochen/Mikoshiba, Katsuhiko/Leinders-Zufall, Trese/Offermanns, Stefan/Schütz, Burkhard/Boehm, Ulrich/Zufall, Frank/Bufe, Bernd/Kummer, Wolfgang (2020). Chemosensory Cell-Derived Acetylcholine Drives Tracheal Muco-

ciliary Clearance in Response to Virulence-Associated Formyl Peptides. Immunity 52 (4), 683-699.e11. https://doi.org/10.1016/j.immuni.2020.03.005.

89. Philippaert, Koenraad/Vennekens, Rudi (2015). Chapter 19 - Transient Receptor Potential (TRP) Cation Channels in Diabetes. In: Arpad Szallasi (Ed.). TRP Channels as Therapeutic Targets. From Basic Science to Clinical Use. Burlington, Elsevier Science, 343–363.

90. Prawitt, Dirk/Monteilh-Zoller, Mahealani K./Brixel, Lili/Spangenberg, Christian/Zabel, Bernhard/Fleig, Andrea/Penner, Reinhold (2003). TRPM5 is a transient Ca2+-activated cation channel responding to rapid changes in Ca2+i. Proceedings of the National Academy of Sciences of the United States of America 100 (25), 15166–15171. https://doi.org/10.1073/pnas.2334624100.

91. Pulce, C./Descotes, J. (1996). 28 - Household products. In: Jacques Descotes (Ed.). Human toxicology. Amsterdam, Elsevier, 683–702.

92. Ricker, Deborah D. (1998). The Autonomic Innervation of the Epididymis: Its Effects on Epididymal Function and Fertility. Journal of andrology 19 (1), 1–4. https://doi.org/10.1002/j.1939-4640.1998.tb02463.x.

93. Riera, Céline E./Vogel, Horst/Simon, Sidney A./Damak, Sami/Le Coutre, Johannes (2009). Sensory attributes of complex tasting divalent salts are mediated by TRPM5 and TRPV1 channels. The Journal of neuroscience : the official journal of the Society for Neuroscience 29 (8), 2654–2662. https://doi.org/10.1523/JNEUROSCI.4694-08.2009.

94. Rinaldi, Vera D./Donnard, Elisa/Gellatly, Kyle/Rasmussen, Morten/Kucukural, Alper/Yukselen, Onur/Garber, Manuel/Sharma, Upasna/Rando, Oliver J. (2020). An atlas of cell types in the mouse epididymis and vas deferens. eLife Sciences Publications, Ltd. Available online at https://elifesciences.org/articles/55474 (accessed 8/23/2020).

95. Robaire, B./Hinton, B./Orgebincrist, M. (2015). The Epididymis. In: Jimmy D. Neill/Ernst Knobil (Eds.). Knobil and Neill's physiology of reproduction. 3rd ed. Amsterdam, Elsevier/Academic Press, 1071–1148.

96. Robaire, Bernard/Hinton, Barry T. (2002). The Epididymis: From Molecules to Clinical Practice. A Comprehensive Survey of the Efferent Ducts, the Epididymis and the Vas Deferens. Boston, MA, Springer US.

97. Saunders, Cecil J./Christensen, Michael/Finger, Thomas E./Tizzano, Marco (2014). Cholinergic neurotransmission links solitary chemosensory cells to nasal inflammation. Proceedings of the National Academy of Sciences 111 (16), 6075–6080. https://doi.org/10.1073/pnas.1402251111.

98. Saunders, Cecil J./Reynolds, Susan D./Finger, Thomas E. (2013). Chemosensory brush cells of the trachea. A stable population in a dynamic epithelium. American journal of respiratory cell and

molecular biology 49 (2), 190–196. https://doi.org/10.1165/rcmb.2012-0485OC.

99. Schünke, Michael/Schulte, Erik/Schumacher, Udo (2015). Innere Organe. Stuttgart, Georg Thieme Verlag.

100. Schütz, Burkhard/Jurastow, Innokentij/Bader, Sandra/Ringer, Cornelia/Engelhardt, Jakob von/Chubanov, Vladimir/Gudermann, Thomas/Diener, Martin/Kummer, Wolfgang/Krasteva-Christ, Gabriela/Weihe, Eberhard (2015). Chemical coding and chemosensory properties of cholinergic brush cells in the mouse gastrointestinal and biliary tract. Frontiers in physiology 6, 87. https://doi.org/10.3389/fphys.2015.00087.

101. Schütz, I./Waldner, M. (2018). „Am Nebenhoden gibt es keinen Krebs.“ Stimmt das? – Komplexe Differentialdiagnosen von malignen Nebenhodentumoren. https://doi.org/10.3205/18nrwgu47.

102. Seiler, P./Wenzel, I./Wagenfeld, A./Yeung, C. H./Nieschlag, E./Cooper, T. G. (1998). The ap-

pearance of basal cells in the developing murine epididymis and their temporal expression of macrophage antigens. International journal of andrology 21 (4), 217–226. https://doi.org/10.1046/j.1365-2605.1998.00116.x.

103. Shah, Alok S./Ben-Shahar, Yehuda/Moninger, Thomas O./Kline, Joel N./Welsh, Michael J. (2009). Motile cilia of human airway epithelia are chemosensory. Science (New York, N.Y.) 325 (5944), 1131–1134. https://doi.org/10.1126/science.1173869.

104. Shi, Jianwu/Fok, Kin Lam/Dai, Pengyuan/Qiao, Feng/Zhang, Mengya/Liu, Huage/Sang, Mengmeng/Ye, Mei/Liu, Yang/Zhou, Yiwen/Wang, Chengniu/Sun, Fei/Xie, Gangcai/Chen, Hao (2021). Spatio-temporal landscape of mouse epididymal cells and specific mitochondria-rich segments defined by large-scale single-cell RNA-seq. Cell discovery 7 (1), 34. https://doi.org/10.1038/s41421-021-00260-7.

105. Shum, Winnie W. C./Hill, Eric/Brown, Dennis/Breton, Sylvie (2013). Plasticity of basal cells during postnatal development in the rat epididymis. Reproduction 146 (5), 455–469. https://doi.org/10.1530/REP-12-0510.

106. Shum, Winnie Wai Chi/Da Silva, Nicolas/McKee, Mary/Smith, Peter J. S./Brown, Dennis/Breton, Sylvie (2008). Transepithelial projections from basal cells are luminal sensors in pseudostratified epithelia. Cell 135 (6), 1108–1117. https://doi.org/10.1016/j.cell.2008.10.020.

107. Shum, Winnie Waichi/Da Silva, Nicolas/Belleannée, Clémence/McKee, Mary/Brown, Dennis/Breton, Sylvie (2011). Regulation of V-ATPase recycling via a RhoA- and ROCKII-dependent pathway in epididymal clear cells. American journal of physiology. Cell physiology 301 (1), C31-43. https://doi.org/10.1152/ajpcell.00198.2010.

108. Silva Júnior da, E. D./Souza, B. P. de/Vilela, V. V./Rodrigues, J. Q. D./Nichi, M./Agostini Losano,

J. D. de/Dalmazzo, A./Barnabe, V. H./Jurkiewicz, A./Jurkiewicz, N. H. (2014). Epididymal contraction and sperm parameters are affected by clonidine. Andrology 2 (6), 955–966. https://doi.org/10.1111/andr.283.

109. Stammler, A./Hau, T./Bhushan, S./Meinhardt, A./Jonigk, D./Lippmann, T./Pilatz, A./Schneider-Hüther, I./Middendorff, R. (2015). Epididymitis: ascending infection restricted by segmental boundaries. Human reproduction (Oxford, England) 30 (7), 1557–1565. https://doi.org/10.1093/humrep/dev112.

110. Sutherland, Kate/Young, Richard L./Cooper, Nicole J./Horowitz, Michael/Blackshaw, L. Ashley (2007). Phenotypic characterization of taste cells of the mouse small intestine. American journal of physiology. Gastrointestinal and liver physiology 292 (5), G1420-8. https://doi.org/10.1152/ajpgi.00504.2006.

111. Talavera, Karel/Yasumatsu, Keiko/Voets, Thomas/Droogmans, Guy/Shigemura, Noriat-

su/Ninomiya, Yuzo/Margolskee, Robert F./Nilius, Bernd (2005). Heat activation of TRPM5 underlies thermal sensitivity of sweet taste. Nature 438 (7070), 1022–1025. https://doi.org/10.1038/nature04248.

112. Talavera, Karel/Yasumatsu, Keiko/Yoshida, Ryusuke/Margolskee, Robert F./Voets, Thomas/Ninomiya, Yuzo/Nilius, Bernd (2008). The taste transduction channel TRPM5 is a locus for bitter-sweet taste interactions. The FASEB Journal 22 (5), 1343–1355. https://doi.org/10.1096/fj.07-9591com.

113. Tizzano, Marco/Gulbransen, Brian D./Vandenbeuch, Aurelie/Clapp, Tod R./Herman, Jake P./Sibhatu, Hiruy M./Churchill, Mair E. A./Silver, Wayne L./Kinnamon, Sue C./Finger, Thomas E. (2010). Nasal chemosensory cells use bitter taste signaling to detect irritants and bacterial signals. Proceedings of the National Academy of Sciences 107 (7), 3210–3215. https://doi.org/10.1073/pnas.0911934107.

114. Trasler, J. M./Hermo, L./Robaire, B. (1988). Morphological changes in the testis and epididymis of rats treated with cyclophosphamide: a quantitative approach. Biology of Reproduction 38 (2), 463–479. https://doi.org/10.1095/biolreprod38.2.463.

115. US Consumer Product Safety Commission (1992). Final Report: Study on Aversive Agents.

116. US Government (Hrsg.) (2006). Epididymis. Available online at https://upload.wikimedia.org/wikipedia/commons/c/c3/Illu_testis_surface.jpg.

117. Vennekens, Rudi/Mesuere, M./Philippaert, K. (2018). TRPM5 in the battle against diabetes and obesity. Acta physiologica (Oxford, England) 222 (2). https://doi.org/10.1111/apha.12949.

118. Wagenlehner, F. M. E./Cek, Mete/Naber, Kurt G./Kiyota, Hiroshi/Bjerklund-Johansen, Truls E. (2012). Epidemiology, treatment and prevention of healthcare-associated urinary tract infections. World journal of urology 30 (1), 59–67. https://doi.org/10.1007/s00345-011-0757-1.

119. Welsch, Ulrich/Deller, Thomas (2011). Sobotta Lehrbuch Histologie. Unter Mitarbeit von Thomas Deller. 3rd ed. s.l., Urban Fischer Verlag - Lehrbücher.

120. Werneburg, Glenn T./Wagenlehner, Florian/Clemens, J. Quentin/Harding, Chris/Drake, Marcus J. (2024). Towards a Reference Standard Definition of Urinary Tract Infection for Research. European Urology Focus. https://doi.org/10.1016/j.euf.2024.09.010.

121. Wiederhold, Stephanie/Papadakis, Tamara/Chubanov, Vladimir/Gudermann, Thomas/Krasteva-Christ, Gabriela/Kummer, Wolfgang (2015). A novel cholinergic epithelial cell with chemosensory traits in the murine conjunctiva. International immunopharmacology 29 (1), 45–50. https://doi.org/10.1016/j.intimp.2015.06.027.

122. Wu, S. Vincent/Chen, Monica C./Rozengurt, Enrique (2005). Genomic organization, expression, and function of bitter taste receptors (T2R) in mouse and rat. Physiological genomics 22 (2),

139–149. https://doi.org/10.1152/physiolgenomics.00030.2005.

123. Xu, Jiang/Cao, Jie/Iguchi, Naoko/Riethmacher, Dieter/Huang, Liquan (2013). Functional characterization of bitter-taste receptors expressed in mammalian testis. Molecular Human Reproduction 19 (1), 17–28. https://doi.org/10.1093/molehr/gas040.

124. Zhang, Yifeng/Hoon, Mark A./Chandrashekar, Jayaram/Mueller, Ken L./Cook, Boaz/Wu, Dianqing/Zuker, Charles S./Ryba, Nicholas J.P. (2003). Coding of Sweet, Bitter, and Umami Tastes. Cell 112 (3), 293–301. https://doi.org/10.1016/S0092-8674(03)00071-0.

10 Declaration

10.1 English version

"I, Dirk Stefan Haas, hereby declare, that I have written this thesis independently and without unauthorized help or use of other than the stated aids. All text passages taken literally or analogously from published or unpublished writings and all information based on verbal information are marked as such. In the research, I conducted and mentioned in the dissertation, I complied with the principles of good scientific practice as laid down in the "Statutes of the Justus-Liebig-University Giessen for Safeguarding Good Scientific Practice", as well as ethical, data protection, and animal welfare principles. I declare, that third parties have not received any payments of monetary value from me, either directly or indirectly, for work related to the content of the dissertation submitted, and that the dissertation submitted has not been submitted in the same or a similar form to any other examination authority, either in Germany or abroad, for the purpose of a doctorate or any other examination procedure. All material taken from other

sources and from other persons, that was used in the thesis or to which direct reference is made, was identified as such. In particular, all persons who were directly or indirectly involved in the creation of this thesis have been named. I agree to my work being checked by plagiarism detection software or an internet-based software program."

Gießen, May 25th, 2025

Dirk Stefan Haas

10.2 German version - Ehrenwörtliche Erklärung

„Hiermit erkläre ich, Dirk Stefan Haas, dass ich die vorliegende Arbeit selbständig und ohne unzulässige Hilfe oder Benutzung anderer als der angegebenen Hilfsmittel angefertigt habe. Alle Textstellen, die wörtlich oder sinngemäß aus veröffentlichten oder nichtveröffentlichten Schriften entnommen sind, und alle Angaben, die auf mündlichen Auskünften beruhen, sind als solche kenntlich gemacht. Bei den von mir durchgeführten und in der Dissertation erwähnten Untersuchungen habe ich die Grundsätze guter wissenschaftlicher Praxis, wie sie in der „Satzung der Justus-Liebig-Universität Gießen zur Sicherung guter wissenschaftlicher Praxis“ niedergelegt sind, eingehalten sowie ethische, datenschutzrechtliche und tierschutzrechtliche Grundsätze befolgt. Ich versichere, dass Dritte von mir weder unmittelbar noch mittelbar geldwerte Leistungen für Arbeiten erhalten haben, die im Zusammenhang mit dem Inhalt der vorgelegten Dissertation stehen, und dass die vorgelegte Arbeit weder im Inland noch im Ausland in gleicher oder ähnlicher Form einer anderen Prüfungsbehörde zum Zweck einer Promotion oder eines ande-

ren Prüfungsverfahrens vorgelegt wurde. Alles aus anderen Quellen und von anderen Personen übernommene Material, das in der Arbeit verwendet wurde oder auf das direkt Bezug genommen wird, wurde als solches kenntlich gemacht. Insbesondere wurden alle Personen genannt, die direkt und indirekt an der Entstehung der vorliegenden Arbeit beteiligt waren. Mit der Überprüfung meiner Arbeit durch eine Plagiatserkennungssoftware bzw. ein internetbasiertes Softwareprogramm erkläre ich mich einverstanden.“

Gießen, 25. Mai 2025

Dirk Stefan Haas

Der Lebenslauf wurde aus der elektronischen Version der Arbeit entfernt.

The curriculum vitae was removed from the electronic version of the paper.

12 Acknowledgements

I would like to thank the following people for supporting this research project:

- Prof. Dr. Ralf Middendorff as my supervisor for his consistent support, patience, and guidance during this project. It has been pleasure learning from him.
- Prof. Dr. Dr. Norbert Krämer for his support as my mentor throughout my studies.
- Sabine Tasch: Without Sabine, I would never be able to complete my research. Her knowledge, skills, and personality are unique. I am proud and grateful to have learned from her and worked with her. I found a nice friend.
- Ludmilla Dorscht: My tutor, who guided me so positively and who always made me feel confident in my abilities after coming off the phone to her.
- Gerrit Eichner for his help with statistics and refreshing my math skills.
- Prof. Dr. Wolfgang Kummer and his team (Dr. Klaus Deckmann, Dr. Alexander Perniß, Dr. Uwe

Pfeil, Tamara Papadakis, Petra Mermer, Silke Wiegand, Martin Bodenbenner) with their advice, especially on the practical experiments.

- Prof. Dr. Andreas Meinhardt, who was my first professor at the faculty of anatomy and who sparked my interest in this field.
- Andrea Mietens for her constant motivation and advice.
- Beatrix Stadler for introducing me to the various procedures at the laboratory. She is an outstanding scientist and always keeps a smile on her face.
- Eva Wewel for helping me from day 1 to feel as a team member.
- Last but not least, without my exam at the age of 55 after 72 months at the dental faculty, I would not be a dentist today. I am proud to have learned so much from all the professors, dentists, doctors, and assistants, including the nice apprentices who helped us students a lot during the challenging times at the dental and university clinics. In particular, there are (in no specific order):

Prof. Dr. Dr. Hans-Peter Howaldt, Prof. Dr. Jörg Meyle, Prof. Dr. Martin Jung, Prof. Dr. Bernd Wöstmann, Prof. Dr. Peter Rehmann, Prof. Dr. Sabine Ruf, Dr. Jens Hermann, Dr. Stephanie Volk, Dr. Kay-Arne Walther, Ghayath Mahfoud, Dr. Sameh Attia, Dr. Andreas May, Dr. Alexander Schmidt, Dr. Katja Jung, Dr. Stefanie Amend, Dr. Nelly Schlulz-Weidner, Dr. Karin Michel, Dr. Kerstin Wegner, Dr. Dr. Sebastian Böttger, Dr. Dr. Michael Knitschke, Dr. Dr. Daniel Schmermund, Dr. Sonja Südwasser, Prof. Dr. Eveline Baumgart-Vogt, Prof. Dr. Ritva Tikannen, Prof. Dr. Michael Niepmann and many more.